Convergent origin and accelerated evolution of vesicle-associated RhoGAP proteins in two unrelated parasitoid wasps

Dominique Colinet*[1], Fanny Cavigliasso[1], Matthieu Leobold[2], Appoline Pichon[3], Serge Urbach[3], Dominique Cazes[1], Marine Poullet[1], Maya Belghazi[4], Anne-Nathalie Volkoff[3], Jean-Michel Drezen[2], Jean-Luc Gatti[1], and Marylène Poirié[1]

[1] Université Côte d'Azur, INRAE, CNRS, ISA, 06903 Sophia Antipolis, France
[2] Institut de Recherche sur la Biologie de l'Insecte (IRBI), UMR 7261, CNRS - Université de Tours, Tours, France
[3] DGIMI, Univ Montpellier, INRAE, 34095 Montpellier, France
[4] Aix Marseille Université, CNRS, Plateforme Protéomique, IMM FR3479, Marseille Protéomique (MaP), 13402 Marseille, France

*Corresponding author
Correspondence: dominique.colinet@inrae.fr

ABSTRACT

Animal venoms and other protein-based secretions that perform a variety of functions, from predation to defense, are highly complex cocktails of bioactive compounds. Gene duplication, accompanied by modification of the expression and/or function of one of the duplicates under the action of positive selection, followed by further duplication to produce multigene families of toxins is a well-documented process in venomous animals. This evolutionary model has been less described in parasitoid wasps, which use maternal fluids, including venom, to protect their eggs from encapsulation by the host immune system. Here, we evidence the convergent recruitment and accelerated evolution of two multigene families of RhoGAPs presumably involved in virulence in two unrelated parasitoid wasp species, *Leptopilina boulardi* (Figitidae) and *Venturia canescens* (Icheumonidae). In both species, these RhoGAPs are associated with vesicles that act as transport systems to deliver virulence factors, but are produced in different tissues: the venom gland in *Leptopilina* sp. and the ovarian calyx in *V. canescens*. We show that the gene encoding the cellular RacGAP1 is at the origin of the virulent RhoGAP families found in *Leptopilina* sp. and *V. canescens*. We also show that both RhoGAP families have undergone evolution under positive selection and that almost all of these RhoGAPs lost their GAP activity and GTPase binding ability due to substitutions in key amino acids. These results suggest an accelerated evolution and functional diversification of these vesicle-associated RhoGAPs in the two phylogenetically distant parasitoid species. The potential new function(s) and the exact mechanism of action of these proteins in host cells remain to be elucidated.

Keywords: parasitoids, venom and other secretions, RhoGAP multigene family, evolution, gene duplication, positive selection

Introduction

Gene duplication is recognized as an important evolutionary process because it drives functional novelty (Chen et al., 2013; Long et al., 2013). The importance of gene duplication for genetic and functional innovation was popularized by Ohno, who postulated that one of the two duplicate copies could evolve a new function through mutation, while the other would be responsible for the ancestral function (Ohno 1970). Since then, there have been numerous examples of duplication followed by neofunctionalization of one of the two paralogs with critical roles in fundamental biological processes (Kaessmann 2010; Magadum et al. 2013, Copley 2020). In particular, the formation of multigene families by repeated gene duplication is a widely studied evolutionary process in several groups of venomous animals (Fry et al., 2009; Wong & Belov 2012; Casewell et al., 2013), but also in some parasites (Akhter et al., 2012; Arisue et al., 2020). Such repeated duplication events of venomous or virulence protein-coding genes are often accompanied by significant copy divergence through positive selection, allowing the acquisition of new functions. In this work, we studied the process of accelerated evolution by duplication and divergence of two multigene families encoding RhoGAPs presumably involved in virulence in two phylogenetically distant parasitoid wasp species, *Leptopilina* species of the family Figitidae and *Venturia canescens* of the family Icheumonidae.

The development of parasitoid wasps occurs at the expense of another arthropod, whose tissues are consumed by the parasitoid larvae, usually resulting in the host death (Godfray 1994). For endoparasitoids that lay eggs inside the host body, the host immune defense against parasitoids is usually based on the formation of a multicellular melanized capsule around the parasitoid egg, resulting in its death (Carton et al., 2008). To escape encapsulation, parasitoids have evolved several strategies, the main one being the injection of maternal fluids together with the egg into the host at the time of oviposition (Pennacchio & Strand 2006; Poirié et al., 2009). These maternal fluids contain (i) proteins synthesized in the venom glands (Asgari & Rivers 2010; Poirié et al., 2014), some of which, as in *Leptopilina,* can be associated with extracellular vesicles called venosomes and allow their transport to the targeted immune cells (Gatti et al., 2012; Wan et al., 2019), (ii) proteins synthesized in the ovarian calyx cells and associated with particles of viral origin devoid of nucleic acid and named virus-like particles (VLPs) as in *V. canescens* (Reineke et al., 2006; Gatti et al., 2012; Pichon et al., 2015), and (iii) polydnaviruses (PDVs) integrated into the parasitoid genome and found in some groups of parasitoids belonging to the families Braconidae and Ichneumonidae (Drezen et al., 2014). Like VLPs, PDVs are synthesized in the ovarian calyx cells and are present in the ovarian fluid along with the egg. These particles are unique in that they are formed by the integrated viral machinery, but carry circular double-stranded DNA molecules that contain virulence genes that will be expressed in the host cells (Drezen et al., 2014). The process of accelerated evolution by duplication and divergence has been described for some of these virulence genes carried by PDVs, suggesting functional diversification of the proteins produced (Serbielle et al., 2008; Serbielle et al., 2012; Jancek et al., 2013).

Leptopilina boulardi is a parasitoid wasp of *Drosophila* for which two lines have been well characterized (Dubuffet et al., 2009). The ISm line of *L. boulardi* is highly virulent against *Drosophila melanogaster* but is unable to develop in *Drosophila yakuba* whereas the ISy line can develop in both *Drosophila* species but its success depends on the resistance/susceptibility of the host (Dubuffet et al., 2009). One of the most abundant proteins in the venom of the *L. boulardi* ISm line is LbmGAP (previously named LbGAP), which belongs to the Rho GTPase activating protein (RhoGAP) family (Labrosse et al., 2005; Colinet et al., 2013). A LbmGAP ortholog named LbyGAP (previously named LbGAPy) is also present in the venom of the *L. boulardi* ISy line, but in lower amounts (Colinet et al., 2010; Colinet et al., 2013). While RhoGAPs are usually intracellular proteins composed of several different domains (Tcherkezian & Lamarche-Vane 2007), LbmGAP and LbyGAP contain only one RhoGAP domain preceded by a signal peptide that allows its secretion. LbmGAP has been shown to be associated with and transported by venosomes to target host hemocytes (Wan et al., 2019). LbmGAP and LbyGAP specifically interact with and inactivate two *Drosophila* Rho GTPases, Rac1 and Rac2 (Colinet et al., 2007; Colinet et al., 2010), which are required for hemocyte proliferation in response to parasitism, hemocyte adhesion around the parasitoid egg, or the formation of intercellular junctions necessary for the capsule formation (Williams et al., 2005; Williams et al., 2006). Combined transcriptomic and proteomic analyses have identified eight additional RhoGAP domain-containing venom proteins in addition to LbmGAP and LbyGAP for both *L. boulardi* lines, suggesting that a multigene family has derived from repeated duplication (Colinet et al., 2013). One of these venom

RhoGAPs, LbmGAP2 (previously named LbGAP2), has also been shown to be associated with venosomes in *L. boulardi* ISm and to be released with LbmGAP in host hemocytes (Wan et al., 2019). Interestingly, three RhoGAP domain-containing venom proteins have also been identified in the closely related species *Leptopilina heterotoma* (Colinet et al., 2013), suggesting that the recruitment of RhoGAPs in the venom arsenal may have occurred before the separation of the two species.

Leptopilina venom RhoGAPs are not the only example of the possible use of a protein from this family in parasitoid virulence (Reineke et al., 2006; Du et al., 2020). In the Ichneumonidae *V. canescens*, a RhoGAP domain-containing protein known as VLP2 (named VcVLP2 in this paper) was found to be associated with VLPs formed in the nucleus of ovarian calyx cells (Reineke et al., 2006; Pichon et al., 2015). VLPs, which package proteic virulence factors wrapped into viral envelopes, are then released into the ovarian lumen to associate with eggs and protect them from the host immune response by as yet unknown mechanisms (Feddersen et al., 1986). Species of the genus *Leptopilina* (superfamily Cynipoidea) as well as *V. canescens* (superfamily Ichneumonoidea) belong to the group of parasitoid wasps, which has been shown to be monophyletic (Peters et al., 2017). They are distantly related, with their last common ancestor dating back to the early radiation of parasitoid wasps, more than 200 million years ago (Peters et al., 2017). The presence of RhoGAP family proteins in the maternal fluids of parasitoid wasps has not been described outside of *Leptopilina* species and *V. canescens*. Overall, these observations suggest convergent recruitment of proteins belonging to the same family and injected into the host with the egg in two phylogenetically distant parasitoid species.

In this work, we showed that VcVLP2 in *V. canescens*, like LbmGAP in *Leptopilina*, is not unique but is part of a multigene family of virulent RhoGAPs associated with extracellular vesicles. RhoGAPs from different organisms are grouped into distinct subfamilies based on similarities in RhoGAP domain sequence and overall multi-domain organization (Tcherkezian & Lamarche-Vane 2007). Our analyses indicate that an independent duplication of the RacGAP1 gene, a member of the large RhoGAP family, was the origin of the two virulent RhoGAP multigene families, one found in *Leptopilina* and the other in *V. canescens*. We then performed comparative analyses to understand the duplication events at the origin of these two virulent RhoGAP multigene families. Finally, we demonstrated evolution under positive selection for both virulent RhoGAP multigene families in *L. boulardi* and *V. canescens,* suggesting accelerated evolution and functional diversification.

Methods

Biological material

The origin of the *L. boulardi* isofemale lines ISm (Lbm; Gif stock number 431) and ISy (Lby; Gif stock number 486) has been described previously (Dupas et al., 1998). Briefly, the ISy and ISm founding females were collected in Brazzaville (Congo) and Nasrallah (Tunisia), respectively. The *L. heterotoma* strain (Lh; GIF stock number 548) was collected in southern France (Gotheron). The Japanese strain of *Leptopilina victoriae* (Lv), described in Novković et al., 2011, was provided by Pr. M. T. Kimura (Hokkaido University, Japan). All parasitoid lines were reared on a susceptible *D. melanogaster* Nasrallah strain (Gif stock number 1333) at 25 °C. After emergence, the wasps were maintained at 20 °C on agar medium supplemented with honey. All experiments were performed on 5- to 10-day-old parasitoid females.

Phylogeny of members of the Cynipoidea superfamily

The phylogeny of selected members of the Cynipoidea superfamily was constructed using internal transcribed spacer 2 (ITS2) sequences available at NCBI (Supplementary Table S1). Multiple sequence alignment was performed using MAFFT with the --auto option (Katoh & Standley 2013). Poorly aligned regions were removed using trimal with the -automated1 option (Capella-Gutierrez et al., 2009). Phylogenetic analysis was performed using maximum likelihood (ML) with IQ-TREE (Minh et al., 2020).

Search for candidate venom RhoGAPs in Leptopilina transcriptomes

L. victoriae venom apparatus, corresponding to venom glands and associated reservoirs, were dissected in Ringer's saline (KCl 182 mM; NaCl 46 mM; $CaCl_2$ 3 mM; Tris-HCl 10 mM). Total RNA was extracted from 100 venom apparatus using TRIzol reagent (Invitrogen) followed by RNeasy Plus Micro Kit (QIAGEN) according to the manufacturers' instructions. The quality of total RNA was checked using an

147 Agilent BioAnalyzer. Illumina RNASeq sequencing (HiSeq 2000, 2 × 75 pb) and trimming were performed
148 by Beckman Coulter Genomics. The raw data are available at NCBI under the BioProject ID PRJNA974978.
149 Sequence assembly was performed using the "RNASeq de novo assembly and abundance estimation with
150 Trinity and cdhit" workflow available on Galaxy at the BIPAA platform (https://bipaa.genouest.org).
151 *Leptopilina clavipes* (whole body), *Ganaspis* sp. G1 (female abdomen), *Andricus quercuscalicis* (whole
152 body) and *Synergus umbraculus* (whole body) transcriptomes were obtained from NCBI under accession
153 numbers GAXY00000000, GAIW00000000, GBNY00000000 and GBWA00000000, respectively. Coding
154 regions in the transcripts were identified and translated using TransDecoder (Haas et al., 2013), which is
155 available on the BIPAA Galaxy platform. Searches for RhoGAP domain-containing sequences in translated
156 coding sequences were performed using hmmsearch from the HMMER package (Eddy 2009) with the
157 RhoGAP (PF00620) HMM profile.

158 **Completion of *L. boulardi* and *L. heterotoma* venom RhoGAP sequences**
159 Venom apparatus, corresponding to venom glands and associated reservoirs, were dissected in Ringer's
160 saline. Total RNA was extracted from venom apparatus using the RNeasy Plus Micro Kit (QIAGEN) according
161 to the manufacturers' instructions. To obtain the full-length coding sequence of LbmGAP1.3, LbmGAP5,
162 LbyGAP6, LhGAP1 and LhGAP2, rapid amplification of cDNA ends (RACE) was performed using the SMART
163 RACE cDNA Amplification Kit (Clontech). For LhGAP3, 3' RACE could not be applied due to the presence of
164 poly(A) stretches in the sequence. LhGAP3-matching sequences were searched for in the transcriptome
165 assembly obtained by Goecks et al., 2013) from the abdomen of *L. heterotoma* females (GenBank accession
166 number GAJC00000000) using the command line NCBI-BLAST package (version 2.2.24). The resulting
167 complete LhGAP3 sequence was then verified by RT-PCR using the iScript cDNA Synthesis Kit (BioRad) and
168 the GoTaq DNA Polymerase (Promega), followed by direct sequencing of the amplified fragment. Geneious
169 software (Biomatters) was used for sequence editing and assembly.

170 **Obtention of Leptopilina RacGAP1 coding sequences**
171 A combination of RT-PCR and RACE using conserved and specific primers was used to clone the full-
172 length ORF sequence of *L. boulardi* ISm and *L. heterotoma* RacGAP1. The amino acid sequence of *Nasonia*
173 *vitripennis* RacGAP1 (Supplementary Table S2) was used to search for similar sequences among
174 Hymenoptera species using BLASTP at NCBI (http://www.ncbi.nlm.nih.gov/blast/). A multiple sequence
175 alignment of the RacGAP1 amino acid sequences found in Hymenoptera was then performed using
176 MUSCLE (Edgar 2004). Two pairs of RacGAP1-specific degenerate primers were designed from the
177 identified conserved regions (Supplementary Figure S1). Total RNA was extracted from Lbm and Lh
178 individuals using the TRIzol reagent (Invitrogen), and RT-PCR experiments were performed using the
179 RacGAP1-specific degenerate primers. After direct sequencing of the amplified fragments, Lbm- and Lh-
180 specific primers were designed to complete the sequences obtained by RT-PCR and RACE (Supplementary
181 Figure S1). The coding sequences of *L. victoriae and L. clavipes* RacGAP1 were obtained by BLAST searches
182 in the corresponding transcriptomes using *L. boulardi* ISm and *L. heterotoma* RacGAP1 sequences as
183 queries.

184 **Obtention of the genomic sequences of Leptopilina venom RhoGAPs and RacGAP1**
185 The genomic sequences of *Leptopilina* venom RhoGAPs and RacGAP1 were obtained by BLAST and
186 Exonerate searches (Slater & Birney 2005) using the corresponding coding sequences as queries. *L. boulardi*
187 ISm, *L. boulardi* ISy, *L. heterotoma* and *L. clavipes* genome assemblies were obtained from NCBI under
188 accession numbers GCA_011634795.1, GCA_019393585.1, GCF_015476425.1 and GCA_001855655.1
189 respectively.

190 **Search for candidate *V. canescens* RhoGAP calyx sequences**
191 Coding regions were identified from the *V. canescens* calyx transcriptome published by Pichon et al.,
192 *(*2015) and translated into protein sequences using TransDecoder (Haas et al., 2013). The search for
193 RhoGAP domain-containing sequences was performed using hmmsearch from the HMMER package (Eddy
194 2009) with the RhoGAP (PF00620) HMM profile. The identified RhoGAP calyx sequences were used as a
195 database for Mascot to explore MS/MS data obtained from purified *V. canescens* VLPs (Pichon et al., 2015)
196 with a false discovery rate of 1%. Only proteins identified by two or more peptides were considered.

197 The *V. Canescens* RacGAP1 coding sequence was obtained by BLAST searches in the *V. canescens* calyx
198 transcriptome using the *N. vitripennis* RacGAP1 sequence as query.
199 The *V. canescens* calyx RhoGAP and RacGAP1 genome sequences were obtained by BLAST and
200 Exonerate searches (Slater and Birney 2005) using the corresponding coding sequences as queries. The *V.*
201 *canescens* genome assembly was obtained from NCBI under accession number GCA_019457755.1.

202 **Identification of domains and motifs and prediction of subcellular localization**
203 The presence and position of signal peptide cleavage sites in the identified RhoGAP domain-containing
204 sequences were predicted using the SignalP server
205 (https://services.healthtech.dtu.dk/service.php?SignalP). The searches for domains and motifs were
206 performed using InterProScan 5 (Jones et al., 2014) on the InterPro integrative protein signature database
207 (https://www.ebi.ac.uk/interpro/). Coiled-coil regions were predicted using COILS (Lucas et al., 1991).
208 Prediction of protein subcellular localization and sorting signals for *Venturia* RacGAP1 and calyx
209 RhoGAPs was performed using the DeepLoc2 server (https://services.healthtech.dtu.dk/services/DeepLoc-
210 2.0/).
211 Nuclear localization for VcRacGAP1 and calyx RhoGAPs was also predicted using the following three
212 tools: NucPred (Brameier et al., 2007) was used to indicate whether a protein spends part of its time in the
213 nucleus (https://nucpred.bioinfo.se/nucpred/), LocTree3 (Goldberg et al., 2014) to provide subcellular
214 localization and Gene Ontology terms (https://rostlab.org/services/loctree3/), and PSORT II (Nakai &
215 Horton 1999) to detect sorting signals and subcellular localization (https://psort.hgc.jp/form2.html).
216 PSORT II results corresponding to ER membrane retention signals and cleavage sites for mitochondrial
217 presequences were included as they may be associated with nuclear localization. Mitochondrial
218 presequences have no sequence homology but possess physical characteristics that allow them to interact
219 with the outer membranes of mitochondria and thus allow the targeting of proteins to the mitochondrial
220 matrix. Regarding mitochondrial targeting, it has been shown from plants to humans that some proteins
221 with mitochondrial presequences are dually targeted to mitochondria and the nucleus (Millar et al., 2006;
222 Mueller et al., 2004). Indeed, anchoring signals to the ER membrane are known to allow baculoviral
223 proteins to migrate to the inner nuclear membrane (Braunagel et al., 1996). Proteins forming VLPs in *V.*
224 *canescens* could thus follow the same pathways as their homologous proteins in baculoviruses, nudiviruses,
225 hytrosaviruses, and bracoviruses due to the conservation of this mechanism among these viruses belonging
226 to the order Lefavirales (Braunagel et al., 1996; Hong et al., 1997; Braunagel et al., 2004; Abd-Alla et al.,
227 2008; Bézier et al., 2009; Braunagel et al., 2009).

228 **Phylogeny of *Leptopilina* venom and *Venturia* calyx RhoGAPs**
229 Searches for *N. vitripennis* RhoGAP sequences were performed using BLASTP at NCBI
230 (http://www.ncbi.nlm.nih.gov/blast/) and hmmsearch from the HMMER package (Eddy 2009) with the
231 RhoGAP (PF00620) HMM profile on the *N. vitripennis* v2 proteome database (Rago et al., 2016).
232 For the phylogenetic analysis of *Leptopilina* venom and *Venturia* calyx RhoGAPs, multiple alignments
233 of the RhoGAP domain amino acid sequences were performed using MAFFT with the --auto option (Katoh
234 and Standley 2013). For codon-based analysis of selection (see below), codon-based alignments of
235 complete coding sequences were performed using RevTrans
236 (https://services.healthtech.dtu.dk/service.php?RevTrans) with the amino acid alignments as templates.
237 Poorly aligned regions were removed using trimAl with the -automated1 option (Capella-Gutierrez et al.,
238 2009). Phylogenetic analyses were performed using maximum likelihood (ML) with IQ-TREE (Minh et al.,
239 2020). ModelFinder was used to select the best model selection for phylogeny (Kalyaanamoorthy et al.,
240 2017).

241 **Codon-based analysis of selection**
242 Codon-based alignments of complete coding sequences were performed with RevTrans using the
243 amino acid alignments as templates (see above). Phylogenetic analyses were performed using maximum
244 likelihood (ML) with PhyML (Guindon et al., 2010). Smart Model Selection was used to choose the best
245 model selection for the phylogeny (Lefort et al., 2017).
246 To detect evolutionary selective pressures acting on RhoGAP sequences, the ratios of non-synonymous
247 substitutions (dN) to synonymous substitutions (dS) were compared using different ML frameworks: the

248 CODEML program in the PAML (Phylogenetic Analysis by Maximum Likelihood) package (Yang 1997; Yang
249 2007), the HyPhy software implemented at http://www.datamonkey.org/ (Delport et al., 2010), and the
250 Selecton server (Stern et al., 2007) available at http://selecton.tau.ac.il/index.html.
251 Five different methods were used to detect codons under positive selection. In the first, codon
252 substitution models implemented in CodeML were applied to the codon-based alignment using the F3x4
253 frequency model. Two pairs of site models were used to determine whether some codons were under
254 positive selection: M1a (neutral) versus M2a (selection) and M7 (beta distribution where $0 < \omega$ (dN/dS
255 ratio) < 1) versus M8 (beta distribution as in M7 with $\omega > 1$ as additional class). The models were compared
256 using a likelihood ratio test (LRT) with 2 degrees of freedom to assess the significance of detection of
257 selection (Yang et al., 2000). Bayes Empirical Bayes (BEB) inference was then used to identify amino acid
258 sites with a posterior probability >95% of being under positive selection (Yang et al., 2005). We then applied
259 four other methods of detection of selection available in the HyPhy package: Single Likelihood Ancestor
260 Counting (SLAC), Fixed Effect Likelihood (FEL), Mixed Effects Model of Evolution (MEME) and Fast Unbiased
261 Bayesian AppRoximation (FUBAR) methods (Kosakovsky Pond & Frost 2005; Murrell et al., 2012; Murrell et
262 al., 2013). To eliminate false-positive detection, only codons identified by CodeML M2a and M8 and at least
263 one of the other methods were considered under positive selection. Radical or conservative replacements
264 were then determined based on whether they involved a change in the physicochemical properties of a
265 given amino acid, such as charge or polarity (Zhang 2000).
266 Four different methods were used to detect codons under negative selection: the Selecton server using
267 the pair of site models M8a (ß & ω=1) versus M8 (ß & ω), and the FEL, SLAC and FUBAR methods mentioned
268 above. Only codons identified by Selecton and at least one other method were considered under purifying
269 selection.
270 To identify specific lineages with a proportion of sites evolving under positive or purifying selection, we
271 performed branch-site REL analyses using the HyPhy package (Kosakovsky Pond et al., 2011). Unlike the
272 branch and branch-site lineage-specific models available in CodeML, branch-site REL does not require *a*
273 *priori* identification of foreground and background branches.

274 **Structural analysis**
275 Molecular modeling of VcVLP2 RhoGAP was performed using the Phyre server with default parameters
276 (http://www.sbg.bio.ic.ac.uk/phyre2/) (Kelley et al., 2015). The model with the highest confidence (100%)
277 and coverage (46%) was obtained using the crystal structure with PDB code 2OVJ as a template. Model
278 quality was evaluated using the QMEAN server (http://swissmodel.expasy.org/qmean/) (Benkert et al.,
279 2011). Briefly, the QMEAN score is a global reliability score with values ranging between 0 (lower accuracy)
280 and 1 (higher accuracy). The associated Z-score relates this QMEAN score to the scores of a non-redundant
281 set of high-resolution X-ray structures of similar size, with ideal values close to 0. Visualization of LbmGAP
282 (Colinet et al., 2007) and VcVLP2 structures and mapping of sites under selection were performed using
283 PyMol (http://sourceforge.net/projects/pymol/). Secondary structure assignment was performed with the
284 DSSP program (Kabsch & Sander 1983). Accessible surface area (ASA) or solvent accessibility of amino acids
285 was predicted using the *ASAView* algorithm (Ahmad et al., 2004).

286 ***In vitro* mutagenesis**
287 The S76K, V124K, L137D, T143L, S150L, I185K, E200G, and V203R mutations were introduced into the
288 LbmGAP cDNA using the QuickChange XL Site-Directed Mutagenesis Kit (Stratagene). The results of *in vitro*
289 mutagenesis were verified by sequencing.

290 **Yeast two-hybrid analysis**
291 Interactions between LbmGAP and LbmGAP mutants and mutated forms of *Drosophila* RhoA, Rac1,
292 Rac2 and Cdc42 GTPases were individually examined by mating as previously described (Colinet et al.,
293 2007). The plasmids expressing the GTPase proteins were tested against the pGADT7-T control vector,
294 which encodes a fusion between the GAL4 activation domain and the SV40 large T-antigen. Reciprocally,
295 plasmids producing LbmGAP and LbmGAP mutants were tested against the pLex-Lamin control vector.
296 Interactions between LbmGAP and the Rac1 and Rac2 GTPases were used as positive controls (Colinet et
297 al., 2007). Interactions were initially tested by spotting five-fold serial dilutions of cells on minimal medium

298 lacking histidine and supplemented with 3-amino-triazole at 0.5 mM to reduce the number of false
299 positives. ß-galactosidase activity was then detected on plates (Fromont-Racine et al., 1997).

300 **Purification of Leptopilina venosomes and mass spectrometry analysis**

301 Twenty-five Lbm, Lby and Lh female venom apparatus were dissected and the reservoirs separated
302 from the gland. The twenty-five reservoirs were then pooled and opened to release the venom content in
303 25 µl of Ringer's solution supplemented with a protease inhibitor cocktail (Sigma). The venom suspension
304 was centrifuged at 500xg for 5 min to remove the residual tissues, then centrifuged at 15,000xg for 10 min
305 to separate the vesicular fraction from the soluble venom proteins (supernatant fraction) (Wan et al.,
306 2019). The vesicular fraction was then washed twice by resuspension in 25 µl of Ringer's solution followed
307 by centrifugation at 15,000xg for 10 min. The two samples were mixed with 4x Laemmli buffer containing
308 ß-mercaptoethanol (v/v) and boiled for 5 min. Proteins were then separated on a 6–16% linear gradient
309 SDS-PAGE and the gel was silver stained as previously described (Colinet et al., 2013). Identification of
310 proteins by nano-LC-tandem mass spectrometry (MS/MS) was performed on bands excised from the gels
311 as previously described (Colinet et al., 2013). MS/MS data analysis was performed with Mascot software
312 (http://www.matrixscience.com), licensed in house using the full-length coding sequences of the
313 *Leptopilina* venom RhoGAP sequences. Data validation criteria were (i) one peptide with individual ion
314 score greater than 50 or (ii) at least two peptides of individual ion score greater than 20. The mascot score
315 is calculated as -10Log (p). The number of peptide matches identified by Mascot software on the MS/MS
316 data was used to determine (i) the number of protein bands in which each venom RhoGAP was found and
317 (ii) the protein band in which each venom RhoGAP was the most abundant. The calculated FDR (based on
318 an automated decoy database search) was less than 1%. The mass spectrometry proteomics data have
319 been deposited to the ProteomeXchange Consortium via the PRIDE (Perez-Riverol et al., 2022) partner
320 repository with the dataset identifier PXD041695.

321 **Results**

322 **Leptopilina venom RhoGAPs probably emerged in the ancestor of the genus**

323 In the Figitidae, venom RhoGAPs have only been described for *L. boulardi* and *L. heterotoma* (Labrosse
324 et al., 2005; Colinet et al., 2013). A search for candidate homologs was performed in the transcriptomes of
325 *L. victoriae* and *L. clavipes*, two other *Leptopilina* species, *Gasnaspis* sp. G1, another member of the family
326 Figitidae, and *Andricus quercuscalicis* and *Synergus umbraculus,* two gall wasp species representatives of
327 the superfamily Cynipoidea outside of Figitidae (separated by approximately 50 Mya (Peters et al., 2017)).
328 The putative venom RhoGAPs were identified based on the presence of a signal peptide at the N-terminus
329 of the protein, followed by a RhoGAP domain (Table 1). Two transcript sequences encoding RhoGAP
330 domain-containing proteins predicted to be secreted were found in *L. victoriae* (LvGAP1 and LvGAP2) and
331 one in *L. clavipes* (LcGAP1), whereas none were found for *Gasnaspis* sp. G1, *A. quercuscalicis* and *S.*
332 *umbraculus* (Table 1 and Figure 1A). Our results therefore suggest that venom RhoGAPs are specific to the
333 genus *Leptopilina* although further taxon sampling would be required to fully support this hypothesis.

334 **Leptopilina venom RhoGAPs likely evolved from a single imperfect duplication of RacGAP1**

335 A phylogenetic analysis was performed to learn more about the evolutionary history of *Leptopilina*
336 venom RhoGAPs. The phylogeny was constructed based on the amino acid sequence of the RhoGAP
337 domain of these venom proteins and that of the 19 RhoGAPs we identified from the predicted proteome
338 of the jewel wasp *Nasonia vitripennis* (Supplementary Table S2). *N. vitripennis* (superfamily Chalcidoidea)
339 was chosen because it was the first parasitoid wasp to have its genome sequenced, and its genome has
340 recently been re-annotated (Rago et al., 2016). Furthermore, the only RhoGAPs found in *N. vitripennis* are
341 classical intracellular RhoGAPs, which are absent in maternal fluids (de Graaf et al., 2010).

342 Prior to phylogenetic analysis, the complete coding sequence was obtained for two Lbm (LbmGAP1.3
343 and LbmGAP5), one Lby (LbyGAP6) and all three Lh venom RhoGAPs as described in the Methods section.
344 Two of the *Leptopilina* venom RhoGAPs, namely LhGAP3 and LcGAP1, were predicted to contain two
345 RhoGAP domains instead of one. Therefore, these two domains were separated for the analysis. The
346 resulting phylogeny identified NvRacGAP1 as the closest RhoGAP from *N. vitripennis* to all *Leptopilina*
347 venom RhoGAPs with confident support values (Figure 1B). Accordingly, the RhoGAP domain found in all

348 *Leptopilina* venom RhoGAPs was predicted to belong to the RacGAP1 subfamily typically found in RacGAP1-
349 related proteins (Table 1). These results suggest that the *Leptopilina* venom RhoGAPs derive from
350 duplication of the *N. vitripennis* RacGAP1 ortholog in *Leptopilina*.

351 **Table 1.** Motif and domain organization of *Leptopilina* venom RhoGAPs. The signal peptide was
352 predicted using SignalP at CBS. The RhoGAP domain (PF00620) from the Pfam database and the
353 RacGAP1 domain (PTHR46199) from the Panther database were identified using InterProScan on the
354 InterPro integrative protein signature database. Compared to Pfam, the Panther database provides
355 information about the specific RhoGAP subfamily to which the domain belongs. Two successive
356 RhoGAP domains were found in LhGAP3 and LcGAP1. Lbm: *L. boulardi* ISm ; Lby: *L. boulardi* ISy ; Lh:
357 *L. heterotoma* ; Lc: *L. clavipes* ; Lv: *L. victoriae.* The dot numbering (e.g., LbmGAP1.1, LbmGAP1.2, and
358 LbmGAP1.3) was used for *Leptopilina* venom RhoGAPs that are encoded by different genes but share
359 high amino acid sequence identity in the RhoGAP domain (greater than 70% identity).

			Signal peptide		RhoGAP domain (PF00620)				RacGAP1 domain (PTHR46199)			
		Total length	From	To	From	To	Length	E-value	From	To	Length	E-value
Lbm	LbmGAP	282	1	20	52	193	142	2.9e-32	38	267	230	7.0e-37
	LbmGAP1.1	292	1	23	58	205	148	1.0e-19	42	255	214	7.0e-30
	LbmGAP1.2	280	1	23	58	205	148	1.1e-19	42	255	214	1.3e-29
	LbmGAP1.3	287	1	23	58	205	148	7.2e-17	42	253	212	1.3e-27
	LbmGAP2.1	251	1	23	44	183	140	9.9e-26	26	234	209	5.5e-37
	LbmGAP2.2	263	1	23	56	196	141	6.6e-26	49	246	198	1.3e-34
	LbmGAP3	295	1	23	56	175	120	3.2e-12	42	266	225	1.2e-27
	LbmGAP4	246	1	20	42	178	137	9.1e-11	38	218	181	5.6e-18
	LbmGAP5	275	1	20	60	207	148	6.3e-23	41	251	211	2.4e-33
Lby	LbyGAP	286	1	20	52	193	142	1.6e-32	38	267	230	3.4e-37
	LbyGAP1.1	287	1	23	58	205	148	5.6e-17	42	255	214	9.9e-28
	LbyGAP1.2	325	1	23	56	203	148	2.9e-17	42	293	252	1.7e-26
	LbyGAP2	256	1	23	44	185	142	8.3e-27	26	234	209	1.5e-37
	LbyGAP3.1	281	1	23	56	175	120	1.8e-11	42	237	196	1.5e-25
	LbyGAP3.2	266	1	23	41	160	120	5.8e-12	28	222	195	6.4e-25
	LbyGAP4	274	1	20	42	177	136	7.4e-09	30	218	189	2.1e-17
	LbyGAP5	275	1	23	60	207	148	4.4e-24	41	251	211	1.2e-35
	LbyGAP6	239	1	20	53	194	142	8.2e-25	49	231	183	9.4e-34
Lh	LhGAP1	293	1	20	43	180	138	5.5e-36	41	289	249	1.0e-38
	LhGAP2	336	1	20	43	181	139	1.5e-29	45	275	231	8.2e-31
	LhGAP3	467	1	20	35	174	140	1.4e-22	34	221	188	1.3e-38
					257	396	140	2.2e-17				
Lc	LcGAP1	497	1	20	43	184	142	3.2e-30				
					249	384	136	3.5e-28	247	478	232	8.46e-71
Lv	LvGAP1	370	1	20	38	179	142	2.4e-30				
	LvGAP2	266	1	20	38	181	144	8.5e-23	33	224	192	3.7e-28

360
361
362 The RacGAP1 coding sequence of *L. boulardi* ISm*, L. heterotoma, L. victoriae and L. clavipes* was
363 obtained either by cloning and sequencing or by searching genomic data, and its domain organization was
364 compared with that of venom RhoGAPs (Figure 1C, Table 1 and Supplementary Figure S2). *Leptopilina*
365 RacGAP1 has a typical domain organization consisting of a coiled-coil region and a C1 motif (protein kinase
366 C-like zinc finger motif, a ~ 50 amino-acid cysteine-rich domain involved in phorbol ester/diacylglycerol and
367 Zn^{2+} binding) followed by a RhoGAP domain (Tcherkezian & Lamarche-Vane 2007). A large part of the
368 RacGAP1 sequence spanning the coiled-coil region and the C1 motif is replaced by the signal peptide in all
369 *Leptopilina* venom RhoGAPs (Figure 1C, Table 1 and Supplementary Figure S2). This suggests that a unique
370 incomplete duplication of the RacGAP1 gene occurred in the ancestor of the *Leptopilina* genus, resulting
371 in a truncated duplicate encoding a RhoGAP with an altered N-terminus.

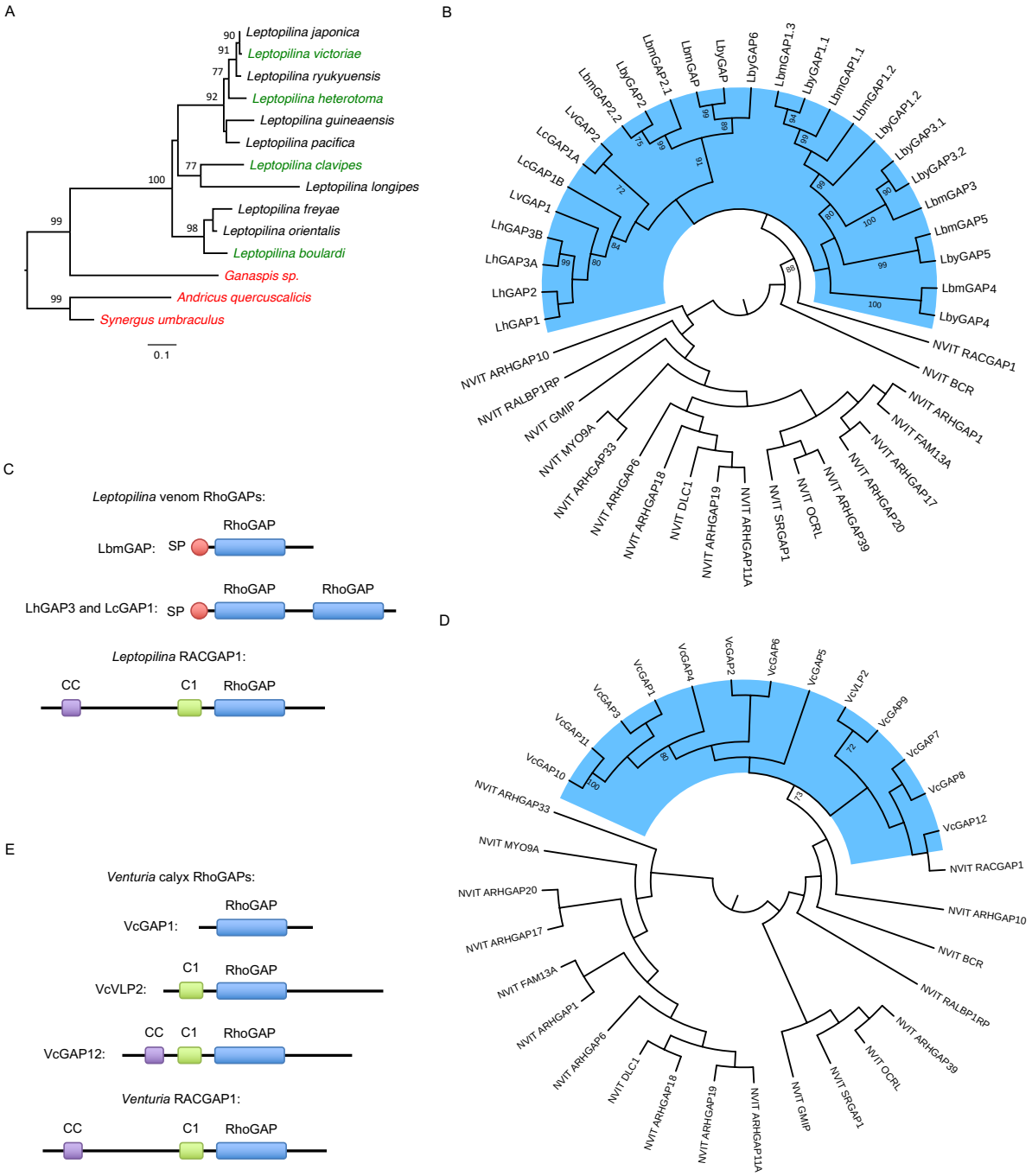

Figure 1. Origin of *Leptopilina* venom RhoGAPs and *Venturia* calyx RhoGAPs (A) Maximum-likelihood phylogenetic tree of selected members of the Cynipoidea superfamily. The phylogenetic tree was obtained with IQ-TREE using internal transcribed spacer 2 (ITS2) sequence. Species in red are those for which venom RhoGAPs were not found. No data were available for species in black. The tree was rooted on the branch that leads to the two gall wasp species, *Andricus quercuscalicis* and *Synergus umbraculus.* The scale bar indicates the number of substitutions per site. (B) Maximum-likelihood phylogenetic tree of *Leptopilina* venom RhoGAPs along with *N. vitripennis* classical RhoGAPs. (C) Comparison of protein domain organization between LbmGAP, representative of most *Leptopilina* venom RhoGAPs, LhGAP3 and LcGAP1, the two venom RhoGAPs that contain two RhoGAP domains, and *Leptopilina* RacGAP1. (D) Maximum-likelihood phylogenetic tree of *Venturia* calyx RhoGAPs along with *N. vitripennis* classical RhoGAPs. (E) Comparison of protein domain organization between VcGAP1, VcVLP2 and VcGAP12, representative of the other *Venturia* calyx RhoGAPs, and *Venturia* RacGAP1. In A, B, and D, numbers at corresponding nodes are bootstrap support values in

386 percent (500 bootstrap replicates). Only bootstrap values greater than 70% are shown. In B and D,
387 the phylogenetic tree was obtained with IQ-TREE using the RhoGAP domain amino acid sequence and
388 displayed as a cladogram. *Leptopilina* venom RhoGAPs and *Venturia* calyx RhoGAPs are highlighted
389 in blue. The tree was rooted at midpoint. In C and E, C1: protein kinase C-like zinc finger motif, CC:
390 coiled-coil region, RhoGAP: RhoGAP domain found in RacGAP1-related proteins, SP: signal peptide.

391 To further investigate this duplication event and the possible origin of the signal peptide, the genomic
392 sequences of *L. boulardi* ISm, *L. heterotoma* and *L. clavipes* venom RhoGAPs and RacGAP1 were obtained,
393 either by cloning and sequencing or by searching in genomic data, and compared (Supplementary Table
394 S3). The genomic sequence of *Leptopilina* RacGAP1 consists of 10 exons with a "CC region", "C1 motif" and
395 "RhoGAP domain" encoded by exons 2 and 3, exons 5 and 6 and exons 7 and 8, respectively. The RhoGAP
396 domain is also encoded by two exons for venom RhoGAPs. These two exons are preceded by one to three
397 exons, with the signal peptide encoded by the first exon for most of them. Sequence comparisons revealed
398 similarities between venom RhoGAPs and *Leptopilina* RacGAP1 only for the sequence spanning the two
399 exons encoding the RhoGAP domain and part of the following one. No significant similarities were found
400 for the preceding exons at either the nucleotide or amino acid level (Supplementary Figure S3). This
401 supports the hypothesis of a partial duplication of the RacGAP1 gene in the ancestor of the *Leptopilina*
402 genus, resulting in the loss of the sequence spanning exons 1 to 6, followed by further duplication of the
403 ancestrally duplicated gene during the diversification of the genus *Leptopilina*.
404 The two consecutive RhoGAP domains found in LhGAP3 were grouped together with confident support
405 values in the phylogenies (Figure 1B and Supplementary Figure S2). This suggests that a partial tandem
406 duplication spanning exons 2 and 3 has occurred for this *L. heterotoma* venom RhoGAP. In contrast, the
407 two RhoGAP domains found in LcGAP1 did not group together (Figure 1B and Supplementary Figure S2).
408 However, the genomic sequence of LcGAP1 was not complete and we could not find the region
409 corresponding to the second RhoGAP domain in the *L. clavipes* genome (Supplementary Table S3).
410 Therefore, it is unclear whether the LcGAP1 coding sequence found in the transcriptome assembly is true
411 or artifactual.

412 ***L. boulardi* and *L. heterotoma* venom RhoGAPs are associated with venosomes**
413 LbmGAP and LbmGAP2 have been shown to be associated with vesicles named venosomes produced
414 in *L. boulardi* venom that transport them to *Drosophila* lamellocytes (Wan et al., 2019). Our next goal was
415 to investigate whether *Leptopilina* venom RhoGAPs other than LbmGAP and LbmGAP2 could be associated
416 with venosomes. Proteomic analysis was performed on the supernatant and vesicular fractions separated
417 from the venom by centrifugation. Comparison of the electrophoretic profiles obtained on a 6-16% SDS-
418 PAGE for *L. boulardi* ISm (Lbm), *L. boulardi* ISy (Lby) and *L. heterotoma* (Lh) revealed an important variation
419 between both fractions for all three wasps (Figure 2). All the major bands on the electrophoretic patterns
420 of Lbm, Lby and Lh supernatant and vesicular fractions, as well as several minor bands (35 bands in total
421 for Lbm, 34 for Lby and 37 for Lh), were excised and tryptic peptides were analyzed by mass spectrometry.
422 The coding sequences of *Leptopilina* venom RhoGAPs were used to perform Mascot searches on the mass
423 spectrometry data obtained from both venom fractions. All *L. boulardi* and *L. heterotoma* venom RhoGAPs
424 were detected in the vesicular fraction, where most of them were found to be enriched (Figure 2). We
425 could then hypothesize that they are associated with and transported by venosomes to target *Drosophila*
426 cells.

A

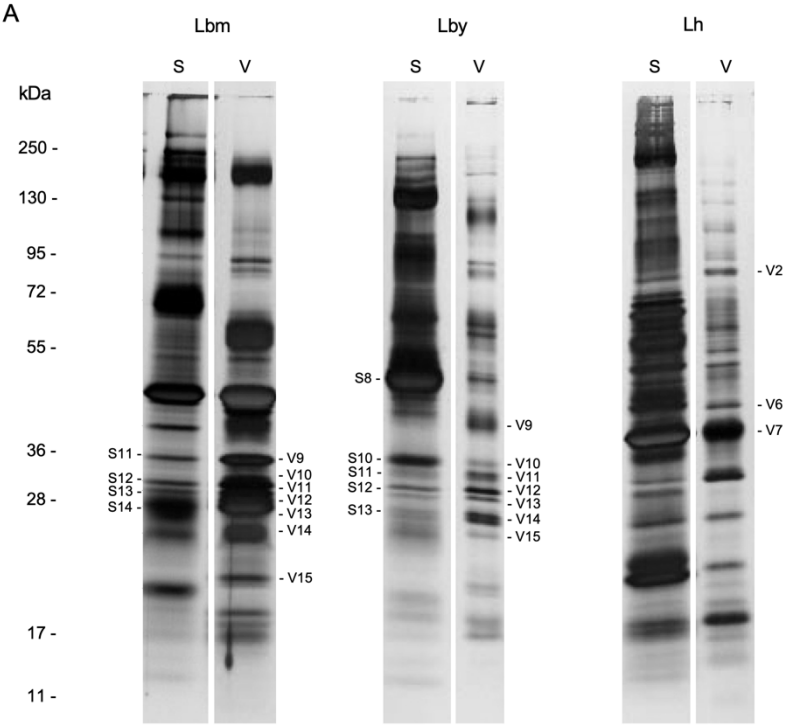

B

				Supernatant		Vesicular	
		Length	Predicted Mw	Protein band	Mascot Matches	Protein band	Mascot Matches
Lbm	LbmGAP	282	32.13	**S11**/S12	11	**V9**/V10/V11/V12/ V13/V14/V15	57
	LbmGAP1.1	292	33.02	S11/**S12**/S14	14	V9/**V10**/V11/V12/ V14/V15	85
	LbmGAP1.2	280	31.99	S13	3	**V10**/**V11**/V12/V13	36
	LbmGAP1.3	287	32.80	S12/**S13**/S14	12	V9/V10/**V11**/V12/ V13/V14/V15	85
	LbmGAP2.1	251	28.81	S11/S12/S13/**S14**	14	V10/V11/V12/ **V13**/V14/V15	60
	LbmGAP2.2	263	30.18	S12/S13/**S14**	9	V9/V10/V11/**V12**/ V13/V14/V15	85
	LbmGAP3	295	34.01	**S12**/S13	3	**V10**/V11/V12/V13	15
	LbmGAP4	246	28.57			V13/**V14**	3
	LbmGAP5	275	31.72			**V10**/V11	10
Lby	LbyGAP	286	32.56	**S8**	1	**V10**/V11	4
	LbyGAP1.1	287	32.81	S10/S11/**S12**/S13	19	V11/**V12**/V13	19
	LbyGAP1.2	325	37.47			**V13**	1
	LbyGAP2	256	29.37	**S8**/S13	8	V12/V13/**V14**	8
	LbyGAP3.1	281	32.58	**S11**	1	V10/**V11**/V12/V13	5
	LbyGAP3.2	266	30.74	**S11**	1	V10/**V11**/V12/V13	5
	LbyGAP4	274	31.92	S10/**S11**/S12/S13	9	V9/V10/**V11**/V12/ V13/V14/V15	36
	LbyGAP5	275	32.04			**V12**	1
	LbyGAP6	239	27.83			**V15**	3
Lh	LhGAP1	293	33.16			**V7**	13
	LhGAP2	336	38.23			**V6**	4
	LhGAP3	467	53.92			**V2**	7

Figure 2. Proteomic analysis of *Leptopilina* venom supernatant and vesicular fractions. (A) The supernatant (S) and vesicular (V) fractions obtained from 25 Lbm, Lby and Lh venom reservoirs were separated on a 6-16% SDS-PAGE under reducing conditions and visualized by silver staining. Protein bands in which *Leptopilina* venom RhoGAPs were identified by mass spectrometry are numbered on the gel. Molecular weight standard positions are indicated on the left (kDa). (B) For each *Leptopilina* venom RhoGAP, length (number of amino acids), predicted Mw (kDa), bands in which specific peptides were found by mass spectrometry and number of total Mascot matches according to the S and V venom fractions are given. Numbers in bold correspond to the bands in which each RhoGAP was identified as the most abundant according to the number of Mascot matches.

437 ***V. canescens* calyx RhoGAPs probably evolved from two or more imperfect RacGAP1 duplication events**

438 Analysis of the *V. canescens* calyx transcriptome allowed the identification of a total of 13 RhoGAP
439 domain-containing protein coding sequences, including VcVLP2 (Table 2 and Supplementary Table S4).
440 Matches with peptides obtained from a proteomic analysis of *V. canescens* VLPs (Pichon et al., 2015) were
441 detected for all 13 calyx RhoGAPs, indicating that they are associated with VLPs (Table 2).

442 Similar to the *Leptopilina* venom RhoGAPs, the *V. canescens* calyx RhoGAPs contain a RacGAP1 domain
443 (Table 2) and are closely related to NvRacGAP1 (Figure 1D). In contrast to the *Leptopilina* venom RhoGAPs,
444 none of the *V. canescens* calyx proteins were predicted to be secreted. Most were predicted to be localized
445 in the nucleus and/or to contain a nuclear localization signal (Supplementary Tables S5 and S6). The
446 absence of a predicted nuclear localization signal for VcGAP7 may be explained by the incomplete coding
447 sequence at the 5' end (Table 2). There is greater variation in domain organization for *V. canescens* calyx
448 RhoGAPs compared to *Leptopilina* venom RhoGAPs (Figure 1E and Supplementary Figure S4). Eight *V.*
449 *canescens* calyx RhoGAPs have retained the C1 motif. In addition, VcGAP12 still contains a CC region in the
450 N-terminal part of the sequence although the total sequence length is shorter than RacGAP1 (Figure 1E
451 and Supplementary Figure S4).

452 **Table 2.** Motif and domain organization of *Venturia* calyx RhoGAP proteins associated with VLPs. The
453 coiled-coil (CC) region was predicted using COILS (Lucas et al., 1991). The protein kinase C-like zinc
454 finger (C1) motif (PS50081) from the Prosite database, the RhoGAP domain (PF00620) from the Pfam
455 database and the RacGAP1 domain (PTHR46199) from the Panther database were identified using
456 InterProScan on the InterPro integrative protein signature database. Compared to Pfam, the Panther
457 database provides information about the specific RhoGAP subfamily to which the domain belongs.
458 Mascot: number of matches with peptides from purified *V. canescens* VLPs. [a]Coding sequence not
459 complete at 5' end. [b]Coding sequence not complete at 3' end.

			CC		C1 (PS50081)		RhoGAP domain (PF00620)				RacGAP1 domain (PTHR46199)			
	Mascot	Total length	From	To	From	To	From	To	Length	E-value	From	To	Length	E-value
VcVLP2	26	485			56	106	134	277	144	7.4e-36	28	366	339	3.1e-98
VcGAP1	9	207					30	168	139	5.7e-25	12	199	188	5.1e-49
VcGAP2	19	280					23	161	139	6.9e-29	8	195	188	1.5e-50
VcGAP3	4	270			22	69	92	231	140	2.6e-25	14	265	252	2.9e-63
VcGAP4	21	382			37	86	116	240	125	2.2e-16	20	298	279	2.7e-68
VcGAP5	19	307			15	63	91	236	146	4.0e-24	7	281	275	2.6e-60
VcGAP6	16	284			17	67	88	215	128	3.3e-19	14	270	257	8.0e-55
VcGAP7	14	225[a]					15	156	142	5.3e-29	4	212	209	9.2e-57
VcGAP8	5	369			64	113	141	281	141	4.6e-28	20	334	315	3.6e-84
VcGAP9	9	319[b]			54	104	123	266	144	1.1e-28	38	306	269	5.5e-73
VcGAP10	5	233					30	166	137	1.6e-22	7	219	213	7.1e-45
VcGAP11	5	199					27	166	140	4.3e-19	8	198	191	5.7e-42
VcGAP12	8	402	21	48	79	131	159	296	138	3.3e-35	54	372	319	9.7e-91

460

461 The genomic coding sequence of VcRacGAP1 was obtained by genomic data mining. It comprised 9
462 exons with the CC region, C1 motif and RhoGAP domain encoded by exons 2 and 3, exons 5 and 6 and exon
463 7, respectively (Supplementary Table S7). In contrast to *Leptopilina*, the RhoGAP domain is encoded by a
464 single exon in *V. canescens* RacGAP1 as well as in all calyx RhoGAPs. Interestingly, the VcGAP12 gene is
465 located close to the VcRacGAP1 gene on chromosome 3, but is three exons shorter, suggesting a recent
466 incomplete duplication (Supplementary Table S7). However, no phylogenetic relationship could be inferred
467 between VcRacGAP1 and VcGAP12, as the corresponding proteins were either grouped in the phylogeny
468 but the grouping was not supported by bootstrap analysis (Figure 1D), or were not grouped in the
469 phylogeny (Supplementary Figure S4). In contrast to VcRacGAP1 and VcGAP12, VcVLP2 and the other
470 VcGAP genes are more widely distributed in the *V. canescens* genome, being organized into several clusters

consisting of two or more genes in tandem arrays (Figure 3 and Supplementary Table S7). For several of these clusters, the *V. canescens* calyx RhoGAP proteins were found in bootstrap-supported groups in the phylogeny, suggesting a close relationship (Figure 1D, Supplementary Figure S4 and Figure 3). This is the case, for example, for VcVLP2 and VcGAP9, VcGAP1 and VcGAP3, or VcGAP10 and VcGAP11, which most likely originated from tandem duplication events. Therefore, it is possible that two or more incomplete duplication events of the VcRacGAP1 gene, followed by further tandem and dispersed duplication of the ancestrally duplicated genes, led to the current number of calyx RhoGAPs in *V. canescens*.

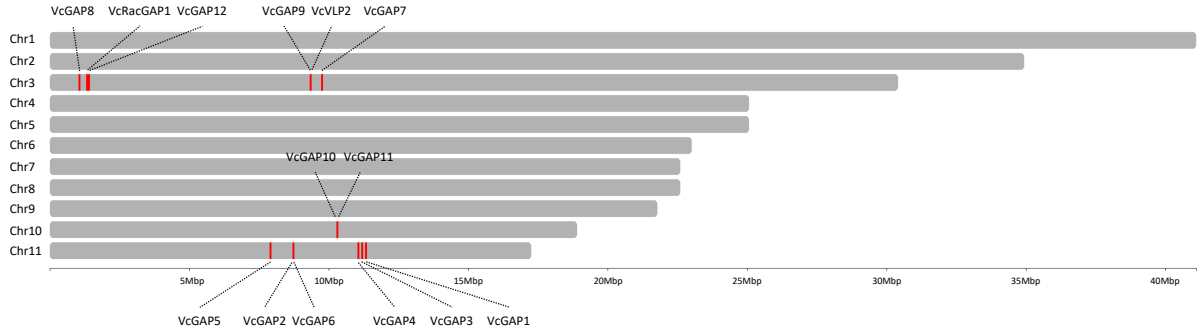

Figure 3. *V. canescens* chromosome map with the position of gene loci corresponding to RacGAP1 and calyx RhoGAPs visualized using chromoMap R package (Anand & Rodriguez Lopez 2022).

Evidence of positive selection in *L. boulardi* venom and *V. canescens* calyx RhoGAP sequences

In a previous work, we identified four amino acid residues involved in the interaction of LbmGAP with Rho GTPases (Colinet et al., 2007), including the key arginine residue (R74 in LbmGAP) required for the GAP catalytic activity (Figure 4A). The other 8 venom RhoGAP sequences found in *L. boulardi* Ism and ISy were all mutated at this arginine residue (Figure 4B). Most also contained substitutions in one or more of the other three amino acids involved in Rho GTPase interaction (Figure 4B). In *V. canescens*, no substitutions were found for VcVLP2 at the key arginine residue or at any of the three amino acids involved in Rho GTPase interaction (Figure 4C). In contrast, all other *V. canescens* calyx RhoGAP sequences, including VcGAP9, for which a close relationship with VcVLP2 could be inferred from phylogenetic analysis and chromosomal location, exhibit substitutions in one or more of the sites essential for GAP activity and/or involved in the interaction with Rho GTPases (Figure 4C). These observations suggest that only LbmGAP (and its ortholog LbyGAP) in *L. boulardi* and VcVLP2 in *V. canescens* are functional as RhoGAPs.

Pairwise sequence identity was lower at the amino acid level than at the nucleotide level for both *Leptopilina* venom RhoGAPs and *V. canescens* calyx RhoGAPs (Supplementary Figure S5). This indicates a higher divergence at non-synonymous sites at the codon level compared to synonymous sites. A search for positive selection at the codon level was performed to detect possible functional divergence of *L. boulardi* venom and *V. canescens* calyx RhoGAP sequences. PAML codon-based models with (M2a and M8) and without (M1a and M7) selection were compared using likelihood ratio tests (LRTs). Both M1a/M2a and M7/M8 comparisons resulted in the rejection of the null hypothesis suggesting that a fraction of codons in RhoGAP sequences are under positive selection (Table 3).

Consistently, a total of 7 and 11 branches of the phylogenetic tree constructed with the *L. boulardi* venom and *V. canescens* calyx RhoGAP sequences, respectively, were detected by the REL branch-site test as corresponding to lineages on which a subset of codons has evolved under positive selection (Figure 5A and 6A). For *L. boulardi*, 6 of the 7 lineages under positive selection were internal branches, indicating that selection occurred primarily before the separation of the *L. boulardi* Ism and ISy strains (Figure 5A).

A

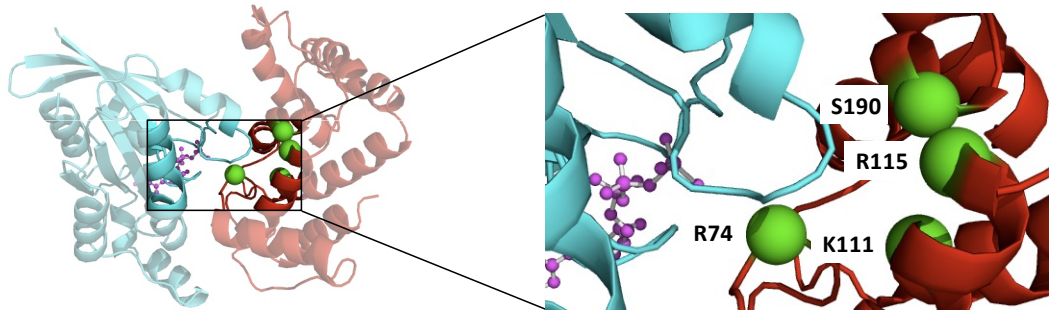

B

		74	111	115	190
	RacGAP1	R	K	R	T
Lbm	LbmGAP	R	K	R	S
	LbmGAP1.1	L	L	S	T
	LbmGAP1.2	L	L	S	I
	LbmGAP1.3	L	L	S	T
	LbmGAP2.1	M	K	R	T
	LbmGAP2.2	M	K	R	T
	LbmGAP3	T	T	R	V
	LbmGAP4	L	V	K	N
	LbmGAP5	L	Q	Y	I
Lby	LbyGAP	R	K	R	S
	LbyGAP1.1	L	L	S	T
	LbyGAP1.2	S	I	S	T
	LbyGAP2	M	K	R	T
	LbyGAP3.1	T	T	R	V
	LbyGAP3.2	T	T	R	V
	LbyGAP4	L	V	K	N
	LbyGAP5	S	Q	Y	I
	LbyGAP6	F	K	R	T

C

		74	111	115	190
	RacGAP1	R	K	R	T
Vc	VcVLP2	R	K	R	T
	VcGAP1	G	K	A	I
	VcGAP2	Q	R	R	A
	VcGAP3	R	K	T	I
	VcGAP4	T	M	K	I
	VcGAP5	S	K	L	V
	VcGAP6	L	K	S	I
	VcGAP7	A	L	R	T
	VcGAP8	Q	K	R	V
	VcGAP9	K	K	R	V
	VcGAP10	R	K	S	I
	VcGAP11	T	K	F	I
	VcGAP12	R	K	A	T

Figure 4. Substitutions in the essential sites for GAP activity and/or involved in interaction with Rho GTPases (A) Tertiary structure of LbmGAP (red) in complex with Rac1 (blue) and the transition-state analogue GDP.AlF3 (modeled by homology for sequence spanning amino acid residues 51 to 216 in Colinet et al., 2007). The four sites essential for GAP activity and/or involved in interaction with RhoGTPases are colored green. (B) Amino acids found at the four sites essential for GAP activity and/or involved in the interaction with RhoGTPases for *Leptopilina* RacGAP1 and *L. boulardi* venom RhoGAP sequences. The numbering corresponds to the positions in the LbmGAP sequence. (C) Amino acids at the four sites essential for GAP activity and/or involved in interaction with RhoGTPases for *V. canescens* RacGAP1 and calyx RhoGAP sequences. The numbering corresponds to the positions in the LbmGAP sequence. In B and C, amino acids are colored according to their properties following the RasMol amino acid color scheme.

Table 3. Positive selection analysis among sites using CodeML for *L. boulardi* venom and *V. canescens* calyx RhoGAP sequences. lnL is the log likelihood of the model. p-value is the result of likelihood ratio tests (LRTs). Global ω is the estimate of the dN/dS ratio under the model (given as a weighted average). Parameters (ω > 1) are parameters estimates for a dN/dS ratio greater than 1 (p is the proportion of sites with ω > 1).

L. boulardi

Model	lnL	p-value	Global ω	Parameters (ω > 1)
M1a: neutral	-5735.55		0.71	
M2a: selection	-5688.59	< 0.001	1.65	ω = 4.70, p = 0.21
M7: ß	-5741.07		0.70	
M8: ß&ω	-5688.19	< 0.001	1.56	ω = 4.4, p = 0.22

V. canescens

Model	lnL	p-value	Global ω	Parameters (ω > 1)
M1a: neutral	-12616.14		0.78	
M2a: selection	-12574.17	< 0.001	1.31	ω = 2.72, p = 0.28
M7: ß	-12612.64		0.73	
M8: ß&ω	-12564.70	< 0.001	1.21	ω = 2.30, p = 0.34

The combined use of five different methods identified a total of 19 codons as candidates under positive selection for the *L. boulardi* venom RhoGAP sequences, most of which were found in the region corresponding to the RhoGAP domain (Figure 5B). In contrast, only 4 amino acids were detected as evolving under negative selection in the *L. boulardi* venom RhoGAPs, respectively (Figure 5C). The leucine at position 9 in LbmGAP is located in the signal peptide, demonstrating the importance of this region. The other three amino acids in *L. boulardi* and most of those in *V. canescens* under negative selection are buried in the protein and are probably important for the structural stability (Figures 5D and 5E and Supplementary Figure S6A).

Interestingly, at least one radical change in charge and/or polarity of the corresponding amino acids was found for all selected codons (Figure 5B). For example, the polar uncharged serine residue at position 76 in LbmGAP was replaced by a negatively charged lysine residue in LbmGAP4 (Figure 5B). Since radical changes are more likely to modify protein function than conservative changes, this suggests that the identified non-synonymous substitutions may be adaptive. Interestingly, the corresponding amino acids are mostly exposed on the surface of the protein and therefore likely to interact with partners (Figures 5D and 5E and Supplementary Figure S6A).

We therefore generated site-specific mutants of LbmGAP for 8 of the 19 amino acids under positive selection and compared their binding capabilities to Rho GTPases. Two-hybrid analysis revealed a lack of interaction for five of the mutants, indicating that the corresponding amino acids are essential for interaction with Rac GTPases (Table 4). On the other hand, the remaining three mutants were still able to interact strongly with Rac1 and Rac2, suggesting that the corresponding amino acids are not involved in the interaction with Rac GTPases (Table 4).

For the *V. canescens* calyx RhoGAP sequences, six amino acids were identified as candidates under positive selection and 19 under negative selection (Figures 5G and 5H). Four of the amino acids under positive selection are predicted to be exposed on the surface of the protein, indicating functional diversification in relation to interaction with partners as in *L. boulardi* (Figures 5I and 5J and Supplementary Figure S6B). Most of the amino acids under negative selection are buried within the protein and are likely to be important for structural stability (Figures 5I and 5J and Supplementary Figure S6B).

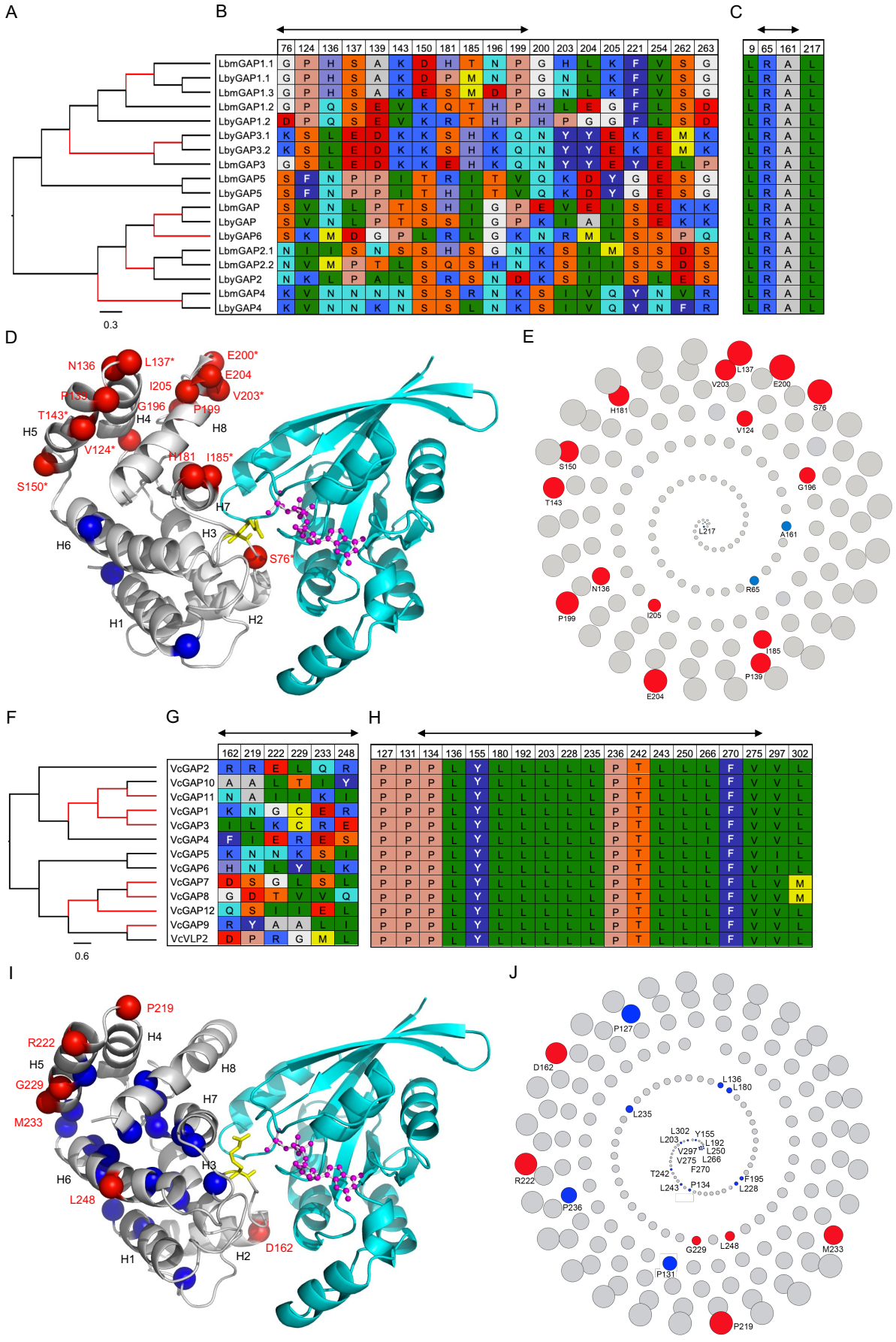
A
B
C
0.3
D
N136
L137*
E200*
E204
I205
V203*
P139
G196
P199
T143*
H4
H8
H5
V124*
H181
I185*
S150*
H7
H3
S76*
H6
H1
H2
E
L137
V203
E200
S76
H181
V124
S150
G196
T143
L217
A161
N136
R65
P199
I205
I185
P139
E204
F
G
H
0.6
I
P219
R222
H4
H5
H8
G229
H7
M233
H3
H6
L248
D162
H1
H2
J
P127
D162
L136
L180
L235
L302
Y155
L203
L192
V297
L250
V275
L266
F270
T242
F195
R222
L243
P134
L228
P236
G229
L248
M233
P131
P219

553 **Figure 5. Identification of branches and codons under selection in *L. boulardi* venom RhoGAPs and**
554 ***V. canescens* calyx RhoGAPs.** (A) Cladogram of *L. boulardi* venom RhoGAPs. (B) Codons under positive
555 selection numbered according to LbmGAP amino acid sequence. (C) Codons under negative selection
556 codons numbered according to LbmGAP amino acid sequence. (D) Sites under positive and negative
557 selection displayed on the tertiary structure of LbmGAP (grey) in complex with Rac1 (blue) and the
558 transition-state analogue GDP.AlF3 (modeled by homology for sequence spanning amino acid
559 residues 51 to 216 in Colinet et al., 2007). A star indicates amino acid residues tested in mutagenesis
560 and two-hybrid interaction assays. (E) Spiral view of LbmGAP amino acids in the order of their solvent
561 accessibility. (F) Cladogram of *V. canescens* calyx RhoGAPs. (G) Codons under positive selection
562 numbered according to VcVLP2 amino acid sequence. (H) Codons under negative selection numbered
563 according to VcvLP2 amino acid sequence. (I) Sites under positive and negative selection displayed
564 on the tertiary structure of VcVLP2 (grey) in complex with Rac1 (blue) and the transition-state
565 analogue GDP.AlF3 (modeled by homology for sequence spanning amino acid residues 117 to 316).
566 (J) Spiral view of VcVLP2 amino acids in the order of their solvent accessibility. In A and F, Branches
567 identified under positive selection by the HyPhy BSR method are colored in red. The cladogram was
568 rooted at midpoint. In B, C, G, and H, amino acids are colored according to their properties following
569 the RasMol amino acid color scheme. The two-sided arrows indicate sites located in the RhoGAP
570 domain. In D and I, the helices are shown as ribbons and numbered according to their location in the
571 amino acid sequence of LbmGAP (D) or VcVLP2 (I). Sites under positive selection are displayed as red-
572 colored spheres and numbered according to the LbmGAP (D) or VcVLP2 (I) sequence. Sites under
573 negative selection are displayed as spheres and colored in blue. Protruding LbmGAP Arg74 (D) and
574 VcVLP2 Arg156 (I) are shown as sticks and colored in yellow. GDP.AlF3 is shown as ball-and-sticks
575 models and colored in magenta. In E and J, Most accessible amino acids come on the outermost ring
576 of the spiral whereas the buried amino acids are occurring in the innermost ring. Radius of the circles
577 corresponds to the relative solvent accessibility. Red and blue colors are used for amino acids under
578 positive and negative selection respectively. All other amino acids are in grey.

579

580 **Table 4.** Summary of the results of interaction assays for the LbmGAP mutants. Results are based on
581 growth on selective medium lacking histidine and qualitative ß-galactosidase overlay assays. -: no
582 interaction; (+): very weak interaction; +++: strong interaction. T: SV40 large T-antigen negative
583 control.

	LbmGAP	LbmGAP S76K	LbmGAP V124K	LbmGAP L137D	LbmGAP T143L	LbmGAP S150L	LbmGAP I185K	LbmGAP E200G	LbmGAP V203R	T
Rac1	+++	-	-	+++	+++	+++	-	-	-	-
Rac2	+++	-	-	+++	+++	+++	-	-	-	-
CDC42	(+)	(+)	(+)	(+)	(+)	(+)	(+)	(+)	(+)	(+)
RhoA	-	-	-	-	-	-	-	-	-	-
Lamin	-	-	-	-	-	-	-	-	-	-

584

585 ## Discussion

586 **Independent convergent recruitment of vesicle-associated RhoGAP proteins in distantly related**
587 **parasitoid species**

588 The process of duplication of a gene encoding a protein usually involved in a key physiological process
589 whose function will be hijacked is a major mechanism of toxin recruitment (Fry et al., 2009; Wong & Belov
590 2012; Casewell et al., 2013). The results of phylogeny and domain analyses indicate that the *Leptopilina*
591 venom RhoGAPs and the calyx RhoGAPs found in *V. canescens* VLPs originated from duplication of the gene
592 encoding the cellular RacGAP1 in these species. This independent convergent recruitment may suggest a
593 similar function in virulence in these two evolutionarily distant parasitoid species. Consistently, our results
594 indicate that venom RhoGAPs in *L. boulardi* and *L. heterotoma* and calyx RhoGAPs in *V. canescens* are
595 associated with extracellular vesicles, named venosomes and VLPs, respectively. While these two types of
596 vesicles have different tissue origins and formation mechanisms, *Leptopilina* venosomes and *V. canescens*
597 VLPs would act as transport systems to deliver virulent proteins, including RhoGAPs, into host hemocytes
598 to alter their function (Pichon et al., 2015; Wan et al., 2019). However, the role of RhoGAPs on host
599 hemocytes is still unclear or even unknown, although we have previously shown that LbmGAP inactivates

600 Rac-like GTPases (Colinet et al., 2007), which are required for successful encapsulation of *Leptopilina* eggs
601 (Williams et al., 2005; Williams et al., 2006).
602 RacGAP1 is an intracellular multidomain protein consisting of a coiled-coil region followed by a C1 motif
603 (protein kinase C-like zinc finger motif) and a RhoGAP domain (Tcherkezian & Lamane-Vane 2007).
604 *Leptopilina* venom RhoGAPs, on the other hand, possess only a RhoGAP domain preceded by a secretory
605 signal peptide. Sequence comparisons at the genomic level support the hypothesis of a single partial
606 duplication of the RacGAP1 gene in the ancestor of the *Leptopilina* genus, resulting in the loss of a 5' portion
607 of the sequence encoding the coiled-coil region and the C1 motif, followed by the acquisition of the signal
608 peptide sequence. This initial evolutionary event would then have been followed by further duplication of
609 the ancestral duplicate gene throughout the diversification of the genus *Leptopilina,* leading to the current
610 number of venom RhoGAPs. A first hypothesis for the origin of the signal peptide would be that the loss of
611 part of the 5' coding sequence in the duplicate resulted in a new N-terminal end for the encoded protein
612 with signal peptide properties. Modification of the N-terminal end of the protein into a fully functional
613 signal peptide may have required some point mutations after partial duplication, as in the case of the
614 antifreeze protein of an Antarctic zoarcid fish (Deng et al., 2010). Another possibility is that the signal
615 peptide originated from a process of partial duplication with recruitment (Katju & Lynch 2006), in which a
616 "proto-peptide signal" coding sequence was acquired from the new genomic environment into which the
617 partial copy was integrated. Finally, it is also possible that the new 5' region of the duplicated copy results
618 from a chimeric duplication (Katju & Lynch 2006), e.g. from the partial duplication of another gene or by
619 exon shuffling (Vibranovski et al., 2006). The acquisition of the signal peptide probably facilitated the
620 neofunctionalization of the venom RhoGAPs according to the evolutionary model of protein subcellular
621 relocalization (PSR) proposed by Byun McKay & Geeta (2007), according to which a modification of the N-
622 or C-terminal region of a protein can change its subcellular localization, by the loss or acquisition of a
623 specific localization signal, and enable it to acquire a new function.
624 In *V. canescens*, the N-terminal region of the calyx RhoGAPs is more variable in length, with some
625 proteins retaining the C1 motif upstream of the RhoGAP domain and one retaining a coiled-coil region
626 upstream of the C1 motif. Most of the *V. canescens* calyx RhoGAPs were predicted to contain a nuclear
627 localization signal, consistent with (i) the accumulation of VcVLP2 in the nucleus of the calyx cells prior to
628 its association with the virus-derived VLPs (Pichon et al., 2015) and (ii) our results from a proteomic analysis
629 indicating that all 13 calyx RhoGAPs are associated with VLPs. Human RacGAP1 has been described to
630 localize to the cytoplasm and nucleus (Mishima et al., 2002), suggesting that *V. canescens* calyx RhoGAPs
631 have retained the RacGAP1 nuclear localization signal, unlike *Leptopilina* venom RhoGAPs. One of the *V.*
632 *canescens* calyx RhoGAP genes is located close to the RacGAP1 gene in the genome, suggesting a recent
633 partial tandem duplication, although without support from phylogenetic analyses. The other genes, on the
634 other hand, are scattered throughout the genome suggesting that they originate from one or more older
635 duplication events of the RacGAP1 gene. In contrast to *Leptopilina*, it cannot be excluded that two or more
636 partial duplication events of the RacGAP1-encoding gene occurred in *V. canescens*, followed by further
637 duplication of ancestral duplicates.

638 **Accelerated evolution through duplication and divergence: pseudogenization and/or**
639 **neofunctionalization?**
640 Our work revealed a significant divergence for the two multigene families of RhoGAPs in *L. boulardi*
641 and *V. canescens* compared to RacGAP1, illustrated by the presence of substitutions on the arginine
642 essential for GAP activity and/or on one or more of the amino acids shown to be important, or even
643 necessary, for interaction with the Rac GTPases in all RhoGAPs except LbmGAP (and its ortholog LbyGAP)
644 and VcVLP2. The presence of substitutions at key sites in the majority of *L. boulardi* venom and *V. canescens*
645 calyx RhoGAPs suggests a loss of function by pseudogenization. However, peptide matches were found in
646 proteomic analyses for each of these RhoGAPs, indicating that the corresponding genes are successfully
647 transcribed and translated. Furthermore, our results indicate that the ancestrally acquired secretory signal
648 peptide, in which we identified an amino acid under negative selection, is conserved in all *L. boulardi*
649 RhoGAPs and that most *V. canescens* RhoGAPs conserved the nuclear localization signal of RacGAP1. In
650 addition, all RhoGAPs retained the ability to associate with vesicles, namely venosomes in *L. boulardi* and
651 VLPs in *V. canescens*. Finally, we showed that several amino acids embedded in the protein structure
652 evolved under negative selection, suggesting that they are important for protein stability. Taken together,

these observations are not consistent with the hypothesis that any of the mutated RhoGAPs is undergoing a pseudogenization process, although it cannot be excluded that this process is quite recent and could have been initiated by the loss of the GAP active site.

An alternative hypothesis to pseudogenization would be functional diversification of the mutated RhoGAPs independent of the Rho pathway. Indeed, we have evidenced an evolution under positive selection for the majority of RhoGAPs in the two multigenic families. Most of the sites under positive selection are located on the surface of the protein and are therefore likely to interact with partners. In addition, directed mutagenesis and two-hybrid experiments in *L. boulardi* have shown that some of these amino acids are not involved in the interaction with Rac GTPases. Although the majority of studies on the RhoGAP domain concern the interaction with Rho GTPases, interactions with other proteins have also been described (Ban et al., 2004; Xu et al., 2013), supporting the hypothesis of a neofunctionalization of the mutated RhoGAPs. Further studies will be needed to determine which functions the mutated RhoGAPs have acquired in relation to parasitism. Recently, a possible role has been proposed for one of the RhoGAPs found in the venom of the ISy line of *L. boulardi* in the induction of reactive oxygen species (ROS) in the central nervous system of *D. melanogaster* in the context of superparasitism avoidance (Chen et al., 2021). However, ROS production is notably regulated by the GTPases Rac1 and Rac2 (Hobbs et al., 2014), whereas this venom protein (named EsGAP1 in Chen et al., 2021 and corresponding to LbyGAP6 in our study) has likely lost its RhoGAP activity due to a substitution on the arginine at position 74. Therefore, the mechanism by which EsGAP1 would be involved in ROS induction is unclear.

Other potential factors involved in parasitic success have been described previously that are encoded by large gene families and similarly correspond to truncated forms of cellular proteins that have retained only a single conserved domain, such as protein tyrosine phosphatases (PTPs) or viral ankyrins (V-ANKs) of bracoviruses. In the case of bracovirus PTPs, some are active as phosphatases, while others are mutated in their catalytic site and have been shown to be inactive as PTPs (Provost et al., 2004). In the latter case, as well as for V-ANK, it has been suggested that by binding to their target, they may act as constitutive inhibitors of the function of the corresponding cellular protein (Provost et al., 2004; Thoetkiattikul et al., 2005). Moreover, the model of adaptive evolution by competitive evolution of duplicated gene copies (Francino 2005) predicts that after a first step in which different copies explore the mutation space, once a protein with an optimal function is obtained, the other copies will begin to decay and undergo pseudogenization. This can lead to intermediate situations where both functional and non-functional proteins are produced, as observed for different virulence protein families of parasitoid wasps. Some of the described features of *L. boulardi* and *V. canescens* RhoGAPs may suggest that a process of competitive evolution is underway in *V. canescens* and *L. boulardi*, although our results are also consistent with the hypothesis of a possible neofunctionalization of these vesicle-associated proteins as discussed above.

In conclusion, we evidenced the independent convergent origin and accelerated evolution of a multigene family of vesicle-associated RhoGAP proteins in two unrelated parasitic wasps. Strikingly, these vesicles, which are similarly involved in parasitism, are produced in distinct organs: the venom apparatus in *Leptopilina* and the ovarian calyx in *V. canescens*. In the case of *Leptopilina* RhoGAPs, the acquisition of a secretory signal peptide after incomplete duplication of the RacGAP1 gene allowed secretion into the venom where the vesicles are formed. *V. canescens* RhoGAPs, on the other hand, probably retained the RacGAP1 nuclear localization signal, because it is in the nucleus of calyx cells that VLPs are formed. Another striking point is that our results suggest a possible functional diversification of vesicle-associated RhoGAPs in both species, with the exception of LbmGAP (and its ortholog LbyGAP) in *L. boulardi* and VcVLP2 in *V. canescens*, which are probably the only ones with RhoGAP activity. An open question would be whether all RhoGAPs are important for parasite success, but by different mechanisms, independent of the Rho pathway or not, depending on whether RhoGAPs are mutated or not.

Acknowledgements

We are highly grateful to Christian Rebuf for help in insects rearing. We also thank Pr. M. T. Kimura (Hokkaido University, Japan) for providing biological material. We would also like to thank Anthony Bretaudeau (INRIA, Rennes, France) for help in the use of the workflows available at the BIPAA platform. We are grateful to the genotoul bioinformatics platform Toulouse Occitanie (Bioinfo Genotoul,

https://doi.org/10.15454/1.5572369328961167E12) and the bioinformatics and genomics platform, BIG, Sophia Antipolis (ISC plantBIOs, https://doi.org/10.15454/qyey-ar89) for computing and storage resources.

Data and supplementary information availability

Raw data from the Illumina RNASeq sequencing of the *L. victoriae* venom apparatus are available at NCBI under the BioProject ID PRJNA974978.

The mass spectrometry proteomics data from *L. boulardi* and *L. heterotoma* venosomes have been deposited to the ProteomeXchange Consortium via the PRIDE (Perez-Riverol et al., 2022) partner repository with the dataset identifier PXD041695.

Supplementary information and material are available online at Data INRAE: https://doi.org/10.57745/K82IWQ

Conflict of interest disclosure

The authors declare that they comply with the PCI rule of having no financial conflicts of interest in relation to the content of the article.

Jean-Luc Gatti and Marylène Poirié are recommenders of PCI Zoology.

Funding

This work was supported by the Department of Plant Health and Environment from INRAE and the French Government (National Research Agency, ANR) through the “Investments for the Future” programs LABEX SIGNALIFE ANR-11-LABX-0028-01 and IDEX UCAJedi ANR-15-IDEX-01.

References

Abd-Alla AM, Cousserans F, Parker AG, Jehle JA, Parker NJ, Vlak JM, Robinson AS, Bergoin M (2008) Genome analysis of a *Glossina pallidipes* salivary gland hypertrophy virus reveals a novel, large, double-stranded circular DNA virus. *Journal of Virology,* **82**, 4595-4611. https://doi.org/10.1128/jvi.02588-07

Anand L, Rodriguez Lopez CM (2022) ChromoMap: an R package for interactive visualization of multi-omics data and annotation of chromosomes. *BMC Bioinformatics,* **23**, 33. https://doi.org/10.1186/s12859-021-04556-z

Ban R, Irino Y, Fukami K, Tanaka H (2004) Human mitotic spindle-associated protein PRC1 inhibits MgcRacGAP activity toward Cdc42 during the metaphase. *Journal of Biological Chemistry,* **279**, 16394-16402. https://doi.org/10.1074/jbc.m313257200

Benkert P, Biasini M, Schwede T (2011) Toward the estimation of the absolute quality of individual protein structure models. *Bioinformatics,* **27**, 343-350. https://doi.org/10.1093/bioinformatics/btq662

Bézier A, Herbinière J, Lanzrein B, Drezen JM (2009) Polydnavirus hidden face: the genes producing virus particles of parasitic wasps. *Journal of Invertebrate Pathology,* **101**, 194-203. https://doi.org/10.1016/j.jip.2009.04.006

Brameier M, Krings A, MacCallum RM (2007) NucPred--predicting nuclear localization of proteins. *Bioinformatics,* **23**, 1159-1160. https://doi.org/10.1093/bioinformatics/btm066

Braunagel SC, Elton DM, Ma H, Summers MD (1996) Identification and analysis of an *Autographa californica* nuclear polyhedrosis virus structural protein of the occlusion-derived virus envelope: ODV-E56. *Virology,* **217**, 97-110. https://doi.org/10.1006/viro.1996.0097

Braunagel SC, Williamson ST, Saksena S, Zhong Z, Russell WK, Russell DH, Summers MD (2004) Trafficking of ODV-E66 is mediated via a sorting motif and other viral proteins: facilitated trafficking to the inner nuclear membrane. *Proceedings of the National Academy of Sciences,* **101**, 8372-8377. https://doi.org/10.1073/pnas.0402727101

Braunagel SC, Cox V, Summers MD (2009) Baculovirus data suggest a common but multifaceted pathway for sorting proteins to the inner nuclear membrane. *Journal of Virology,* **83**, 1280-1288. https://doi.org/10.1128/jvi.01661-08

750 Byun McKay SA, Geeta R (2007) Protein subcellular relocalization: A new perspective on the origin of novel
751 genes. *Trends in Ecology & Evolution*, **22**, 338–344. https://doi.org/10.1016/j.tree.2007.05.002
752 Capella-Gutierrez S, Silla-Martinez JM, Gabaldon T (2009) trimAl: a tool for automated alignment trimming
753 in large-scale phylogenetic analyses. *Bioinformatics,* **25**, 1972-1973.
754 https://doi.org/10.1093/bioinformatics/btp348
755 Carton Y, Poirié M, Nappi AJ (2008) Insect immune resistance to parasitoids. *Insect Science,* **15**, 67-87.
756 https://doi.org/10.1111/j.1744-7917.2008.00188.x
757 Casewell NR, Wüster W, Vonk FJ, Harrison RA, Fry BG (2013) Complex cocktails: the evolutionary novelty
758 of venoms. *Trends in Ecology & Evolution,* **28**, 219-229. https://doi.org/10.1016/j.tree.2012.10.020
759 Chen S, Krinsky BH, Long M (2013) New genes as drivers of phenotypic evolution. *Nature Reviews Genetics,*
760 **14**, 645-660. https://doi.org/10.1038/nrg3521
761 Chen J, Fang G, Pang L, Sheng Y, Zhang Q, Zhou Y, Zhou S, Lu Y, Liu Z, Zhang Y, Li G, Shi M, Chen X, Zhan S,
762 Huang J (2021) Neofunctionalization of an ancient domain allows parasites to avoid intraspecific
763 competition by manipulating host behaviour. *Nature Communications,* **12**, 5489.
764 https://doi.org/10.1038/s41467-021-25727-9
765 Colinet D, Schmitz A, Depoix D, Crochard D, Poirié M (2007) Convergent use of RhoGAP toxins by eukaryotic
766 parasites and bacterial pathogens. PloS Pathog **3**: e203. https://doi.org/10.1371/journal.ppat.0030203
767 Colinet D, Schmitz A, Cazes D, Gatti J-L, and Poirié M (2010) The origin of intraspecific variation of virulence
768 in an eukaryotic immune suppressive parasite. *PLoS Pathogens,* **6**, e1001206.
769 https://doi.org/10.1371/journal.ppat.1001206
770 Colinet D, Deleury E, Anselme C, Cazes D, Poulain J, Azema-Dossat C, Belghazi M, Gatti J-L, Poirié M (2013)
771 Extensive inter- and intraspecific venom variation in closely related parasites targeting the same host:
772 the case of *Leptopilina* parasitoids of *Drosophila*. *Insect Biochemistry and Molecular Biology,* **43**, 601–
773 611. https://doi.org/10.1016/j.ibmb.2013.03.010
774 Copley SD (2020) Evolution of new enzymes by gene duplication and divergence. *FEBS Journal*, **287**, 1262-
775 1283. https://doi.org/10.1111/febs.15299.
776 de Graaf DC, Aerts M, Brunain M, Desjardins CA, Jacobs FJ, Werren JH, Devreese B (2010) Insights into the
777 venom composition of the ectoparasitoid wasp *Nasonia vitripennis* from bioinformatic and proteomic
778 studies. *Insect Molecular Biology*, **19**, 11-26. https://doi.org/10.1111/j.1365-2583.2009.00914.x
779 Deng C, Cheng C-HC, Ye H, He X, Chen L (2010) Evolution of an antifreeze protein by neofunctionalization
780 under escape from adaptive conflict. *Proceedings of the National Academy of Sciences,* **107**, 21593-
781 21598. https://doi.org/10.1073/pnas.1007883107
782 Delport W, Poon AF, Frost SD, Kosakovsky Pond SL (2010) Datamonkey 2010: A suite of phylogenetic
783 analysis tools for evolutionary biology. *Bioinformatics,* **26**, 2455-2477.
784 https://doi.org/10.1093/bioinformatics/btq429
785 Drezen J-M, Chevignon G, Louis F, Huguet E (2014) Origin and evolution of symbiotic viruses associated
786 with parasitoid wasps. *Current Opinion in Insect Science*, **6**, 35-43.
787 https://doi.org/10.1016/j.cois.2014.09.008
788 Du J, Lin Z, Volovych O, Lu Z, Zou Z (2020) A RhoGAP venom protein from *Microplitis mediator* suppresses
789 the cellular response of its host *Helicoverpa armigera*. *Developmental & Comparative Immunology,* **108**,
790 103675. https://doi.org/10.1016/j.dci.2020.103675
791 Dupas S, Frey F, Carton Y (1998) A single parasitoid segregating factor controls immune suppression in
792 *Drosophila*. *Journal of Heredity,* **89**, 306-311. https://doi.org/10.1093/jhered/89.4.306
793 Edgar RC (2004) Muscle: multiple sequence alignment with high accuracy and high throughput. *Nucleic*
794 *Acids Research,* **32**, 1792–1797. https://doi.org/10.1093/nar/gkh340
795 Eddy SR (2009) A new generation of homology search tools based on probabilistic inference. *Genome*
796 *Informatics,* **23**, 205–211. https://doi.org/10.1142/9781848165632_0019
797 Feddersen I, Sander K, Schmidt O (1986) Virus-like particles with host protein-like antigenic determinants
798 protect an insect parasitoid from encapsulation. *Experientia,* **42**, 1278-1281.
799 https://doi.org/10.1007/BF01946422
800 Francino MP (2005) An adaptive radiation model for the origin of new gene functions. *Nature Genetics,* **37**,
801 573-577. https://doi.org/10.1038/ng1579
802 Fromont-Racine M, Rain JC, Legrain P (1997) Toward a functional analysis of the yeast genome through
803 exhaustive two-hybrid screens. *Nature Genetics,* **16**, 277–282. https://doi.org/10.1038/ng0797-277

804 Fry BG, Roelants K, Champagne DE, Scheib H, Tyndall JDA, King GF, Nevalainen TJ, Normann JA, Lewis RJ,
805 Norton RS, Renjifo D, Rodriguez de la Vega RC (2009) The toxicogenomic multiverse: convergent
806 recruitment of proteins into animal venoms. *Annual Review of Genomics and Human Genetics,* **10**, 483–
807 511. https://doi.org/10.1146/annurev.genom.9.081307.164356
808 Gatti J-L, Schmitz A, Colinet D, Poirié M (2012) Diversity of virus-like particles in parasitoids' venom: viral
809 or cellular origin? In: Beckage NE, Drezen J-M, editors, Parasitoid viruses, pp. 181–192, London:
810 Academic Press. https://doi.org/10.1016/B978-0-12-384858-1.00015-1
811 Godfray HCJ (1994) Parasitoids: behavioral and evolutionary ecology (Vol. 67): Princeton University Press.
812 https://doi.org/10.2307/j.ctvs32rmp
813 Goecks J, Mortimer NT, Mobley JA, Bowersock GJ, Taylor J, Schlenke TA (2013) Integrative approach reveals
814 composition of endoparasitoid wasp venoms. *PLoS One,* **8**, e64125.
815 https://doi.org/10.1371/journal.pone.0064125
816 Goldberg T, Hecht M, Hamp T, Karl T, Yachdav G, Ahmed N, Altermann U, Angerer P, Ansorge S, Balasz K,
817 Bernhofer M, Betz A, Cizmadija L, Do KT, Gerke J, Greil R, Joerdens V, Hastreiter M, Hembach K, Herzog
818 M, Kalemanov M, Kluge M, Meier A, Nasir H, Neumaier U, Prade V, Reeb J, Sorokoumov A, Troshani I,
819 Vorberg S, Waldraff S, Zierer J, Nielsen H, Rost B (2014) LocTree3 prediction of localization. *Nucleic Acids*
820 *Research,* **42**, W350-355. https://doi.org/10.1093/nar/gku396
821 Guindon S, Dufayard JF, Lefort V, Anisimova M, Hordijk W, Gascuel O (2010) New algorithms and methods
822 to estimate maximum-likelihood phylogenies: assessing the performance of PhyML 3.0. *Systematic*
823 *Biology,* **59**, 307–321. https://doi.org/10.1093/sysbio/syq010
824 Haas BJ, Papanicolaou A, Yassour M, Grabherr M, Blood PD, Bowden J, Couger MB, Eccles D, Li B, Lieber M,
825 MacManes MD, Ott M, Orvis J, Pochet N, Strozzi F, Weeks N, Westerman R, William T, Dewey CN,
826 Henschel R, LeDuc RD, Friedman N, Regev A (2013) De novo transcript sequence reconstruction from
827 RNA-seq using the Trinity platform for reference generation and analysis. *Nature Protocols,* **8**, 1494–
828 1512. https://doi.org/10.1038/nprot.2013.084
829 Hobbs GA, Zhou B, Cox AD, Campbell SL (2014) Rho GTPases, oxidation, and cell redox control. *Small*
830 *GTPases,* **5**, e28579. https://doi.org/10.4161/sgtp.28579
831 Hong T, Summers MD, Braunagel SC (1997) N-terminal sequences from *Autographa californica* nuclear
832 polyhedrosis virus envelope proteins ODV-E66 and ODV-E25 are sufficient to direct reporter proteins
833 to the nuclear envelope, intranuclear microvesicles and the envelope of occlusion derived virus.
834 *Proceedings of the National Academy of Sciences,* **94**, 4050-4055.
835 https://doi.org/10.1073/pnas.94.8.4050
836 Jancek S, Bézier A, Gayral P, Paillusson C, Kaiser L, Dupas S, Le Ru BP, Barbe V, Periquet G, Drezen J-M,
837 Herniou E A (2013) Adaptive selection on bracovirus genomes drives the specialization of *Cotesia*
838 parasitoid wasps. *PLoS One*, **8**, e64432. https://doi.org/10.1371/journal.pone.0064432
839 Jones P, Binns D, Chang H-Y, Fraser M, Li W, McAnulla C, McWilliam H, Maslen J, Mitchell A, Nuka G, Pesseat
840 S, Quinn AF, Sangrador-Vegas A, Scheremetjew M, Yong S-Y, Lopez R, Hunter S (2014) InterProScan 5:
841 genome-scale protein function classification. *Bioinformatics*, **30**, 1236–1240.
842 https://doi.org/10.1093/bioinformatics/btu031
843 Kabsch W, Sander C (1983) Dictionary of protein secondary structure: pattern recognition of hydrogen-
844 bonded and geometrical features. *Biopolymers,* **22**, 2577-2637.
845 https://doi.org/10.1002/bip.360221211
846 Kalyaanamoorthy S, Minh BQ, Wong TKF, von Haeseler A, Jermiin LS (2017) ModelFinder: fast model
847 selection for accurate phylogenetic estimates. *Nature Methods,* **14**, 587–589.
848 https://doi.org/10.1038/nmeth.4285
849 Katju V, Lynch M (2006) On the formation of novel gene by duplication in the *Caenorhabditis elegans*
850 genome. *Molecular Biology and Evolution,* **23**, 1056–1067. https://doi.org/10.1093/molbev/msj114
851 Katoh K, Standley DM (2013) MAFFT multiple sequence alignment software version 7: Improvements in
852 performance and usability. *Molecular Biology and Evolution,* **30**, 772–780.
853 https://doi.org/10.1093/molbev/mst010
854 Kelley LA, Mezulis S, Yates CM, Wass MN, Sternberg MJ (2015) The Phyre2 web portal for protein modeling,
855 prediction and analysis. *Nature Protocols,* **10**, 845-858. https://doi.org/10.1038/nprot.2015.053
856 Kolde R (2019) pheatmap: Pretty Heatmaps. R package version 1.0.12. https://CRAN.R-
857 project.org/package=pheatmap

Kosakovsky Pond SL, Frost SD (2005) Not so different after all: a comparison of methods for detecting amino acid sites under selection. *Molecular Biology and Evolution,* **22**, 1208-1222. https://doi.org/10.1093/molbev/msi105

Kosakovsky Pond SL, Murrell B, Fourment M, Frost SD, Delport W, Scheffler K (2011) A random effects branch-site model for detecting episodic diversifying selection. *Molecular Biology and Evolution,* **28**, 3033-3043. https://doi.org/10.1093/molbev/msr125

Labrosse C, Stasiak K, Lesobre J, Grangeia A, Huguet E, Drezen J-M, Poirié M (2005) A RhoGAP protein as a main immune suppressive factor in the *Leptopilina boulardi* (Hymenoptera, Figitidae)-*Drosophila melanogaster* interaction. *Insect Biochemistry and Molecular Biology,* **35**, 93–103. https://doi.org/10.1016/j.ibmb.2004.10.004

Lefort V, Longueville J-E, Gascuel O (2017) SMS : Smart model selection in PhyML. *Molecular Biology and Evolution,* **34**, 2422-2424. https://doi.org/10.1093/molbev/msx149

Long M, VanKuren NW, Chen S, Vibranovski MD (2013) New gene evolution: little did we know. *Annual Review of Genetics,* **47**, 307-333. https://doi.org/10.1146/annurev-genet-111212-133301

Lucas A, Van Dyke M, Stock J (1991) Predicting coiled coils from protein sequences. *Science*, **252**, 1162-1164. https://doi.org/10.1126/science.252.5009.1162

Magadum S, Banerjee U, Murugan P, Gangapur D, Ravikesavan R (2013) Gene duplication as a major force in evolution. Journal of genetics, 92, 155-61. https://doi.org/10.1007/s12041-013-0212-8.

Millar AH, Whelan J, Small I (2006) Recent surprises in protein targeting to mitochondria and plastids. *Current Opinion in Plant Biology,* **9**, 610-615. https://doi.org/10.1016/j.pbi.2006.09.002

Minh BQ, Schmidt HA, Chernomor O, Schrempf D, Woodhams MD, von Haeseler A, Lanfear R (2020) IQ-TREE 2: New models and efficient methods for phylogenetic inference in the genomic era. *Molecular Biology and Evolution,* **37**, 1530–1534. https://doi.org/10.1093/molbev/msaa015

Mishima M, Kaitna S, Glotzer M (2002) Central spindle assembly and cytokinesis require a kinesin-like protein/RhoGAP complex with microtubule bundling activity. *Developmental Cell,* **2**, 41–54. https://doi.org/10.1016/s1534-5807(01)00110-1

Mueller JC, Andreoli C, Prokisch H, Meitinger T (2004) Mechanisms for multiple intracellular localization of human mitochondrial proteins. *Mitochondrion,* **3**, 315-325. https://doi.org/10.1016/j.mito.2004.02.002

Murrell B, Wertheim JO, Moola S, Weighill T, Scheffler K, Kosakovsky Pond SL (2012) Detecting individual sites subject to episodic diversifying selection. *PLoS Genetics,* **8**, e1002764. https://doi.org/10.1371/journal.pgen.1002764

Murrell B, Moola S, Mabona A, Weighill T, Sheward D, Kosakovsky Pond SL, Scheffler K (2013) FUBAR: A fast, unconstrained bayesian approximation for inferring selection. *Molecular Biology and Evolution,* **30**, 1196-1205. https://doi.org/10.1093/molbev/mst030

Nakai K, Horton P (1999) PSORT: a program for detecting sorting signals in proteins and predicting their subcellular localization. *Trends in Biochemical Sciences,* **24**, 34-36. https://doi.org/10.1016/s0968-0004(98)01336-x

Novković B, Mitsui H, Suwito A, Kimura MT (2011) Taxonomy and phylogeny of *Leptopilina* species (Hymenoptera: Cynipoidea: Figitidae) attacking frugivorous drosophilid flies in Japan, with description of three new species. *Entomological Science,* **14**, 333–346. https://doi.org/10.1111/j.1479-8298.2011.00459.x

Ohno S (1970) Evolution by gene duplication. Springer Verlag, Berlin. https://doi.org/10.1007/978-3-642-86659-3

Pennacchio F, Strand MR (2006) Evolution of developmental strategies in parasitic Hymenoptera. *Annual Review of Entomology,* **51**, 233–258. https://doi.org/10.1146/annurev.ento.51.110104.151029

Perez-Riverol Y, Bai J, Bandla C, Hewapathirana S, García-Seisdedos D, Kamatchinathan S, Kundu D, Prakash A, Frericks-Zipper A, Eisenacher M, Walzer M, Wang S, Brazma A, Vizcaíno JA (2022). The PRIDE database resources in 2022: A Hub for mass spectrometry-based proteomics evidences. *Nucleic Acids Research,* **50**, D543-D552. https://doi.org/10.1093/nar/gkab1038

Peters RS, Krogmann L, Mayer C, Donath A, Gunkel S, Meusemann K, Kozlov A, Podsiadlowski L, Petersen M, Lanfear R, Diez PA, Heraty J, Kjer KM, Klopfstein S, Meier R, Polidori C, Schmitt T, Liu S, Zhou X, Wappler T, Rust J, Misof B, Niehuis O (2017) Evolutionary history of the Hymenoptera. *Current Biology,* **27**, 1013-1018. https://doi.org/10.1016/j.cub.2017.01.027

Pichon A, Bézier A, Urbach S, Aury J-M, Jouan V, Ravallec M, Guy J, Cousserans F, Thézé J, Gauthier J, Demettre E, Schmieder S, Wurmser F, Sibut V, Poirié M, Colinet D, da Silva C, Couloux A, Barbe V, Drezen J-M, Volkoff A-N (2015) Recurrent DNA virus domestication leading to different parasite virulence strategies. *Science Advances,* 1, e1501150. https://doi.org/10.1126/sciadv.1501150

Poirié M, Carton Y, Dubuffet A (2009) Virulence strategies in parasitoid Hymenoptera as an example of adaptive diversity. *Comptes Rendus Biologies,* **332**, 311–320. https://doi.org/10.1016/j.crvi.2008.09.004

Poirié M, Colinet D, Gatti J-L (2014) Insights into function and evolution of parasitoid wasp venoms. *Current Opinion in Insect Science,* **6**, 52–60. https://doi.org/10.1016/j.cois.2014.10.004

Provost B, Varricchio P, Arana E, Espagne E, Falabella P, Huguet E, La Scaleia R, Cattolico L, Poirié M, Malva C, Olszewski JA, Pennacchio F, Drezen JM (2004) Bracoviruses contain a large multigene family coding for protein tyrosine phosphatases. *Journal of Virology,* **78**, 13090-13103. https://doi.org/10.1128/jvi.78.23.13090-13103.2004

Rago, A, Gilbert DG, Choi J-H, Sackton TB, Wang X, Kelkar YD, Werren JH, Colbourne JK (2016) OGS2: genome re-annotation of the jewel wasp *Nasonia vitripennis*. *BMC Genomics,* **17**, 678. https://doi.org/10.1186/s12864-016-2886-9

Reineke A, Asgari S, Schmidt O (2006) Evolutionary origin of *Venturia canescens* virus-like particles. *Archives of Insect Biochemistry and Physiology,* **61**, 123–133. https://doi.org/10.1002/arch.20113

Serbielle C, Chowdhury S, Pichon S, Dupas S, Lesobre J, Purisima E, Drezen J-M, Huguet E (2008) Viral cystatin evolution and three-dimensional structure modelling: a case of directional selection acting on a viral protein involved in a host-parasitoid interaction. *BMC Biology,* **6**, 38. https://doi.org/10.1186/1741-7007-6-38

Serbielle C, Dupas S, Perdereau E, Héricourt F, Dupuy C, Huguet E, Drezen, J-M (2012) Evolutionary mechanisms driving the evolution of a large polydnavirus gene family coding for protein tyrosine phosphatases. *BMC Ecology and Evolution,* **12**, 253. https://doi.org/10.1186/1471-2148-12-253

Sievers F, Higgins DG (2018) Clustal Omega for making accurate alignments of many protein sequences. *Protein Science*, **27**, 135-145. https://doi.org/10.1002/pro.3290

Slater GSC, Birney E (2005) Automated generation of heuristics for biological sequence comparison. *BMC Bioinformatics,* **6**, 31. https://doi.org/10.1186/1471-2105-6-31

Stern A, Doron-Faigenboim A, Erez E, Martz E, Bacharach E, Pupko T (2007) Selecton 2007: advanced models for detecting positive and purifying selection using a Bayesian inference approach. *Nucleic Acids Research,* **35**(Web Server issue), W506-511. https://doi.org/10.1093/nar/gkm382

Tcherkezian J, Lamarche-Vane N (2007). Current knowledge of the large RhoGAP family of proteins. *Biology of the Cell,* **99**, 67–86. https://doi.org/10.1042/bc20060086

Thoetkiattikul H, Beck MH, Strand MR (2005) Inhibitor kappaB-like proteins from a polydnavirus inhibit NF-kappaB activation and suppress the insect immune response. *Proceedings of the National Academy of Sciences,* **102**, 11426-11431. https://doi.org/10.1073/pnas.0505240102

Vibranovski MD, Sakabe NJ, de Souza SJ (2006) A possible role of exon-shuffling in the evolution of signal peptides of human proteins. *FEBS Letters,* **580**, 1621–1624. https://doi.org/10.1016/j.febslet.2006.01.094

Wan B, Goguet E, Ravallec M, Pierre O, Lemauf S, Volkoff A-N, Gatti J-L, Poirié M (2019) Venom atypical extracellular vesicles as interspecies vehicles of virulence factors involved in host specificity: the case of a drosophila parasitoid wasp. *Frontiers in Immunology,* **10**, 1688. https://doi.org/10.3389/fimmu.2019.01688

Wickham H (2009) Ggplot2: Elegant graphics for data analysis. 2nd Edition, Springer, New York. https://doi.org/10.1007/978-0-387-98141-3

Wickham H, François R, Henry L, Müller K, Davis Vaughan (2023) dplyr: A grammar of data manipulation. R package version 1.1.0. https://CRAN.R-project.org/package=dplyr

Williams MJ, Ando I, Hultmark D (2005) *Drosophila melanogaster* Rac2 is necessary for a proper cellular immune response. *Genes to Cells*, **10**, 813–823. https://doi.org/10.1111/j.1365-2443.2005.00883.x

Williams MJ, Wiklund ML, Wikman S, Hultmark D (2006) Rac1 signalling in the *Drosophila* larval cellular immune response. *Journal of Cell Science,* **119**, 2015–2024. https://doi.org/10.1242/jcs.02920

Wong ESW, Belov K (2012) Venom evolution through gene duplications. *Gene,* **13**, 59–69. https://doi.org/10.1016/j.gene.2012.01.009

966 Xu J, Zhou X, Wang J, Li Z, Kong X, Qian J, Hu Y, Fang J-Y (2013) RhoGAPs attenuate cell proliferation by
967 direct interaction with p53 tetramerization domain. *Cell Reports,* **3**, 1526-1538.
968 https://doi.org/10.1016/j.celrep.2013.04.017
969 Yang Z (1997) PAML: a program package for phylogenetic analysis by maximum likelihood. *Bioinformatics,*
970 **13**, 555-556. https://doi.org/10.1093/bioinformatics/13.5.555
971 Yang Z (2007) PAML 4: phylogenetic analysis by maximum likelihood. *Molecular Biology and Evolution,* **24**,
972 1586-1591. https://doi.org/10.1093/molbev/msm088
973 Yang Z, Nielsen R, Goldman N, Pedersen AM (2000) Codon-substitution models for heterogeneous
974 selection pressure at amino acid sites. *Genetics,* **155**, 431-449.
975 https://doi.org/10.1093/genetics/155.1.431
976 Yang Z, Wong WS, Nielsen R (2005) Bayes empirical bayes inference of amino acid sites under positive
977 selection. *Molecular Biology and Evolution,* **22**, 1107–1118. https://doi.org/10.1093/molbev/msi097
978 Zhang J (2000) Rates of conservative and radical nonsynonymous nucleotide substitutions in mammalian
979 nuclear genes. *Journal of Molecular Evolution,* **50**, 56–68. https://doi.org/10.1007/s002399910007